SOME ASPECTS OF NONLINEAR OPTICS

by

MANOJ JAIN

A dissertation submitted to the Graduate Faculty in Physics in partial fulfillment of the requirements for the degree of Doctor of Philosophy, The City University of New York.

1976

This manuscript has been read and accepted for the Graduate Faculty in Physics in satisfaction of the dissertation requirement for the degree of Doctor of Philosophy.

Aug. 4, 1976
date

Narkis Tzoar
Prof. Narkis Tzoar
Chairman of Examining Committee

August 4, 1976
date

Myriam P. Sarachik
Prof. Myriam Sarachik
Executive Officer

Prof. Joel I. Gersten

Robert Alfano
Prof. Robert Alfano

George Skorinko
Prof. George Skorinko

Hyatt M. Gibbs
Dr. Hyatt M. Gibbs

Supervisory Committee

The City University of New York

Acknowledgements

I wish to express my sincere gratitude to Prof. Narkis Tzoar for his constant inspiration and guidance throughout the course of this work. I thank him especially for his patience with me and his ability to provide me with basic physical insight into complex physical phenomena.

I gratefully acknowledge the help and guidance of Prof. Joel I. Gersten and want to thank him for many illuminating discussions relating to this research.

I am also grateful to Prof. Robert Alfano for the kind interest shown in this work. The stimulating and thought provoking atmosphere provided by the City College Faculty must also be acknowledged. Finally, I would like to thank all my fellow Graduate students for providing laughter and sunshine during my stay at City College.

TABLE OF CONTENTS

CHAPTER I

Introduction

As a consequence of the invention of powerful lasers, a new frontier has been opened up in physics. This is understandable because the electric fields generated by these lasers are comparable to the intrinsic fields existing in matter on the atomic scale. Then the response of the materials to the laser fields can no longer be treated in a linear way. This has lead to the interesting field of nonlinear optics. A host of nonlinear phenomena have been discovered and the nonlinear optical processes continue to be the object of intensive investigation.

Historically, nonlinear optics goes back to the discovery of optical second harmonic generation by Franken et al[1] in 1961. Since then, new nonlinear effects have been discovered at a tremendously rapid rate. These include sum- and difference- frequency generation[1-6], parametric amplification and oscillations[2-6], self-focusing[7,8], self induced transparency[9,10], self phase modulation[11,12], multiphoton absorption[13-15], stimulated scattering[16,17] etc. Their potential usefulness was immediately recognized and nonlinear optics has become an important branch in the ever expanding field of quantum optics.

Lately, developements in tunable lasers and ultrashort pulsed lasers have further helped in expanding the studies of nonlinear optics to a wide range of different media. A better understanding of the nonlinear interaction of radiation with matter should result in both scientific and technological

advances in applications of high power lasers to laboratory and industry and in construction of useful nonlinear optical devices. Over the past years, this field has been reviewed constantly by researchers in the form of books[18-22] and review articles[23-26].

In this work, we have been concerned with some aspects of nonlinear optics dealing with propagation of intense laser light in narrow gap semiconductors. The typical semiconductor that has been considered is InSb. The reason for this choice is its low energy gap (0.234 eV) and low effective electron mass (1/60 electron mass). As will be shown later, this results in InSb displaying a large nonlinear behaviour with the result that the nonlinear effects would be observable even with moderately high laser intensities. The nonlinearity could be further enhanced by appropriate use of a dc magnetic field to obtain cyclotron resonance. Then, due to nonlinear effects, the propagation of laser radiation in the semiconductor would be radically different than in the linear regime. The three nonlinear effects that are considered here are self-focusing, self-induced transparency and four photon parametric amplification.

In Chapter II , we extend[27] the previous work[28] on self-focusing in narrow gap semiconductors to include a dc magnetic field and show that this will result in a large enhancement in the self-focusing of laser light. This effect should be extremely useful for injecting a very intense field into a limited region in a crystal.

The propagation of intense optical pulses through the semiconductor is considered in Chapter III. Here we study[29] the nonlinear reflection

properties and modes of propagation in which the spreading tendency for a pulse due to dispersion is compensated for by the compression tendency caused by nonlinear effects. This problem has potential usefulness in the design of lightwave transmission lines and thus is of technological importance.

Finally in Chapter IV, we discuss[30] a four photon parametric process resulting from the nonlinear interaction of intense light from two laser sources propagating in a semiconductor imbedded in dc magnetic field. This process is found to be usefulfor obtaining a tunable device which would be a new type of laser source in a frequency domain, like far infrared , not currently available.

In conclusion, in this work, some aspects of nonlinear optics are studied and it is shown that the results obtained are useful for a better understanding of the basic physics of the nonlinear interaction of radiation with matter, have technological applications and can be used to construct a useful optical device.

CHAPTER II

Magnetic Field Enhancement of Self-Focusing of Laser Beams in Semiconductors

A. Introduction

In a laser beam , in general , the light intensity is not uniform along the profile of the beam, being maximum at the center and tapering off to zero along the edges. When the dielectric properties of the conducting medium are functions of the laser beam intensity, a sort of optical inhomogenity is set up in the presence of the beam and can result in the medium behaving as a focusing lens. This effect termed as self-focusing has received much attention both theoretically and experimentally [31-36]. Several mechanisms for self-focusing has been discussed, among them the Kerr effect, electrostriction, thermal perturbation of the sample, nonlinear electronic polarization and forward stimulated Brillouin scattering.

Recently two new mechanisms which exist in semiconductors have been proposed. The first one[28] results from the large nonparabolicity of the conduction band for narrow-gap semiconductors. Here the nonlinearity arises because of the velocity dependent mass of the conduction electrons. The second [37,38] makes use of the energy dependent collision time for the conduction electrons in semiconductors, due to their interaction with longitudinal optic phonons.

In this chapter, we discuss the self-focusing phenomenon in a

narrow gap semiconductor embedded in a uniform magnetic field. We take the velocity dependent mass to be the dominant contributor to the nonlinear dielectric response of the medium. The effect of the magnetic field on the nonlinearity becomes enormous when the laser frequency ω and the cyclotron frequency ω_c are of the same order of magnitude. Then the electrons and the electric field vector of the circularly polarized light are rotating in space almost coherently and the light accelarates the electrons to a much higher velocity than in the absence of the magnetic field. This results in a large increase in the nonlinear properties of the semiconductor.

The main limitation on the electron accelaration is the collision time τ .Here we are limited to the case when ω , ω_c and $\omega-\omega_c$ are much larger than τ^{-1}. Moreover, the photon mean free path decreases with increasing magnetic field, which we overcome, in part, by decreasing the electron densities. It is the effects on self-focusing resulting from (i) the increase of the nonlinearity and (ii) the decrease of the mean free path of the photon as a function of the magnetic field strength and the laser intensity that are mainly considered here. We find that for realistic situations, self-focusing in the presence of a magnetic field can be achieved with laser powers one to two orders of magnitude smaller than without the magnetic field.

Self-focusing effects become important whenever one is interested in transmitting intense radiation through a crystal. Thus it could play an

important role in such experiments as parametric conversion, harmonic generation, self-induced transparency and laser design studies. In addition self-focusing provides with a procedure for injecting a very large field, especially in the presence of a magnetic field, into a limited region in a crystal. This could lead to interesting studies of the dynamics of hot conduction electrons or generation of lattice imperfections. By studying the self-focusing profile, it is possible to draw conclusions about the nonlinear dielectric constant of the sample.

In section B , we derive an expression for the nonlinear dielectric constant in the presence of a magnetic field. Section C concerns itself with the conditions required for the self-focusing of a radiation beam and in section D, numerical results and a discussion of these results are presented.

B. Calculation of the Nonlinear Dielectric Function

We consider a semiconductor such as InSb , GaAs etc. with electron density n in the conduction band. It is assumed that n is sufficiently small that collective effects play a negligible role. Also the crystal anisotropy will be neglected. As shown by Kane[39] , the dynamics of these electrons, owing to their interaction with the lattice is given to a high degree of accuracy by the Hamiltonian,

$$H_o = \left[(E_g/2)^2 + E_g p^2/2m^* \right]^{1/2} \tag{2.1}$$

Here E_g is the gap energy separating the bottom of the conduction band from the top of the valence band, m^* is the effective mass of the electron near the band's bottom, and p is the electronic momentum. As we go to higher momentum, Eq.(2.1) becomes less accurate, but we will be confined to fairly low values of p .

If we define

$$c^* = \left(E_g/2m^* \right)^{1/2} \tag{2.2a}$$

the Hamiltonian in Eq.(2.1) becomes

$$H_o = \left[m^{*2}c^{*4} + c^{*2}p^2 \right]^{1/2} \tag{2.2b}$$

which formally resembles that of a relativistic electron. Here c^* plays the same role in the dynamics of electrons that the speed of light c plays in relativistic mechanics. For realistic situations $c^*/c \ll 1$.

As we will be interested only in the long-wavelength response of the semiconductor we will not resort to quantum mechanical description.

It is to be noted that in a relativistic situation the velocity and momentum are not linearly related. Whereas the electronic current is proportional to the velocity, the temporal evolution of the momentum is governed linearly by the electromagnetic field. Thus we have a nonlinear dependence of the current on the field.

We now consider the electron dynamics when the semiconductor is imbedded in a uniform magnetic field $\vec{B}_o$ taken to point along the $-z$ direction. In addition we irradiate the sample with circularly polarized light whose direction is directed along the magnetic field. The Hamiltonian then becomes

$$H = \left[m^{*2} c^{*4} + c^{*2} \left(\vec{P} + \frac{e}{c} \vec{A} \right)^2 \right]^{1/2} \tag{2.3}$$

where the vector potential is given by

$$\vec{A} = \frac{1}{2} \vec{B}_o \times \vec{r} + A_1 \left[\hat{i} \cos(\xi - \chi) + \hat{j} \sin(\xi - \chi) \right] \tag{2.4}$$

Here $\xi = kz - \omega t$ and χ is a constant phase angle. Hamilton's equations then lead to the following equations of motion for the electron:

$$\frac{d}{dt} \left[\frac{m^* \vec{v}}{\left[1 - (v/c^*)^2 \right]^{1/2}} \right] = -e \left[\vec{E} + \frac{\vec{v}}{c} \times \vec{B} \right] \tag{2.5}$$

where $\vec{E} = -\frac{1}{c} \frac{\partial \vec{A}}{\partial t}$ and $\vec{B} = \nabla \times \vec{A}$.

In order to account for the effects of electron collisions we introduce a phenomenological relaxation term into Eq.(2.5). Thus we obtain

$$\left(\frac{d}{dt} + \frac{1}{\tau} \right) m^* \vec{v} \Gamma = -e \left[\vec{E} + \frac{\vec{v}}{c} \times \vec{B} \right] \qquad (2.6)$$

where

$$\Gamma = \left[1 - (v/c^*)^2 \right]^{-\frac{1}{2}} \qquad (2.7)$$

This is a realistic model for the carrier densities and field intesities considered in these calculations.

Eq. (2.6) will be solved in the following approximation. We note that the ac magnetic field induces currents which are typically a factor of v/c smaller than the currents induced by the ac electric field. Since $v < c^*$ and c^* is roughly two orders of magnitude smaller than c, we neglect the ac magnetic force and simply replace $\vec{B}$ by $\vec{B}_0$ in Eq. (2.6). In principle we can go to very large values of $\vec{B}_0$ and thus the static field plays an important role in the electron dynamics. Hence we obtain the following set of equations :

$$\left(\frac{d}{dt} + \frac{1}{\tau} \right) m^* v_x \Gamma = \frac{e\omega A_1}{c} \sin(\xi - \chi) + \frac{e}{c} B_0 v_y \qquad (2.8a)$$

$$\left(\frac{d}{dt} + \frac{1}{\tau} \right) m^* v_y \Gamma = -\frac{e\omega A_1}{c} \cos(\xi - \chi) - \frac{e}{c} B_0 v_x \qquad (2.8b)$$

$$\left(\frac{d}{dt} + \frac{1}{\tau} \right) m^* v_z \Gamma = 0 \qquad (2.8c)$$

In the absence of any perturbation the electron gas can be approximated as a cold plasma. Thus the initial velocity $\vec{v} = 0$.

We now investigate the steady state solution to Eqs. (2.8a)-(2.8c). Let $V_x = V_0 \cos(\xi - \chi - \varphi)$ and $V_y = V_0 \sin(\xi - \chi - \varphi)$. From Eq.(2.8c) it immediately follows that $V_z = 0$. The values of φ and v_0 follow directly upon inserting the above forms into Eq.(2.8). They are determined by equating the real and imaginary parts of

$$\omega - \frac{\omega_c}{\Gamma} + \frac{i}{\tau} = \frac{e A_1 \omega e^{i\varphi}}{m^* c \Gamma V_0} \tag{2.9}$$

where, we have introduced the zero-field cyclotron frequency $\omega_c = \frac{eB_0}{m^* c}$.

We note that $\Gamma = (1 - V_0^2/c^{*2})^{-\frac{1}{2}}$ and is independent of time. Thus we find

$$\varphi = \tan^{-1}\left[1/(\omega - \bar{\omega}_c)\tau\right] \tag{2.10a}$$

$$V_0 = \omega \alpha c^* \frac{\bar{\omega}_c}{\omega_c} \frac{1}{\Delta} \tag{2.10b}$$

where, we have introduced a dimensionless parameter $\alpha = eA_1/m^* c^* c$ denoting the strength of the field;

$$\Delta = \sqrt{(\omega - \bar{\omega}_c)^2 + 1/\tau^2} \tag{2.10c}$$

which is a term describing the detuning from resonance; and a renormalized cyclotron frequency

$$\bar{\omega}_c = \omega_c \left[1 - \frac{V_0^2}{c^{*2}}\right]^{1/2} \tag{2.10d}$$

Eq. (2.10a)-(2.10d) must be solved self-consistently to obtain v_0.

In what follows, we will always work with parameters such that $\omega\tau >> 1$ and $(\omega - \omega_c)\tau >> 1$. From Eq. (2.10d) we deduce that $(\omega - \bar{\omega}_c)\tau >> 1$. Consequently the phase shift of Eq. (2.10a) will be small.

The current density associated with the electronic motion is given by,

$$\vec{J} = -ne\vec{v}$$

$$= -nev_0\left[\hat{i}\cos(\xi - \chi - \varphi) + \hat{j}\sin(\xi - \chi - \varphi)\right] \quad (2.11)$$

One notes from Eqs. (2.10a)-(2.10d) that v_0 depends on the field strength parameter in a highly nonlinear way. Thus Eq. (2.11) describes the nonlinear response to the external field. This current acts as the source term in the wave equation,

$$\nabla^2\vec{A} - \frac{\epsilon_L}{c^2}\frac{\partial^2\vec{A}}{\partial t^2} = -\frac{4\pi}{c}\vec{J} \quad (2.12)$$

where ϵ_L is the dielectric constant for the lattice.

We now examine the plane wave solution to Eq. (2.12). Since the current lags behind the vector potential by a phase φ , there will be attenuation of the wave as it propagates through the medium. As a first approximation one can regard $\vec{A}_1$ as being attenuated exponentially with damping constant β ,

$$\vec{A}_1(z) = \vec{A}_1 e^{i(\xi - \chi)} e^{-\beta z}$$

Upon inserting the above equation into Eq. (2.12) and equating the real and imaginary parts, we obtain the following for β and k ,

$$\left(\beta^2 - k^2 + \frac{\epsilon_L \omega^2}{c^2}\right)^2 + 4\beta^2 k^2 = \left(\frac{4\pi n e v_0}{c A_1}\right)^2 \tag{2.13a}$$

$$\frac{2\beta k}{\beta^2 - k^2 + \epsilon_L \frac{\omega^2}{c^2}} = \tan\varphi \tag{2.13b}$$

Solving Eqs. (2.13) simultaneously and using the results obtained in Eqs. (2.10) gives,

$$\left(\beta^2 - k^2 + \epsilon_L \frac{\omega^2}{c^2}\right) \frac{\Delta}{\omega - \bar{\omega}_c} = \frac{\omega_p^2}{c^2} \epsilon_L \frac{\omega}{\Delta} \frac{\bar{\omega}_c}{\omega_c} \tag{2.14a}$$

$$2\beta k \Delta\tau = \frac{\omega_p^2}{c^2} \epsilon_L \frac{\omega}{\Delta} \frac{\bar{\omega}_c}{\omega_c} \tag{2.14b}$$

Substituting for k from Eq. (2.14b) into Eq. (2.14a) gives us a quadratic equation for β^2:

$$\beta^4 + \beta^2 \left[\epsilon_L \frac{\omega^2}{c^2} - (\omega - \bar{\omega}_c) \frac{\omega_p^2}{c^2} \epsilon_L \frac{\omega}{\Delta^2} \frac{\bar{\omega}_c}{\omega_c}\right] - \left[\frac{1}{2\tau} \frac{\omega}{\Delta^2} \frac{\omega_p^2}{c^2} \epsilon_L \frac{\bar{\omega}_c}{\omega_c}\right]^2 = 0$$

On solving for β^2, the above equation gives,

$$\beta^2 = \frac{\omega^2 \epsilon_L}{2c^2} \left[-1 + \left(1 - \frac{\bar{\omega}_c}{\omega}\right) \frac{\omega_p^2}{\Delta^2} \frac{\bar{\omega}_c}{\omega_c} + \left\{1 - 2\left(1 - \frac{\bar{\omega}_c}{\omega}\right) \frac{\omega_p^2}{\Delta^2} \frac{\bar{\omega}_c}{\omega_c} + \frac{\omega_p^4}{\Delta^2 \omega^2} \frac{\bar{\omega}_c^2}{\omega_c^2}\right\}^{1/2}\right] \tag{2.15}$$

For large τ , we can approximate Δ by $(\omega - \bar{\omega}_c)$ and the above equation reduces to

$$\beta^2 = \frac{\omega^2 \epsilon_L}{2c^2}\left[-1 + \frac{\omega_p^2}{\omega(\omega-\bar{\omega}_c)}\frac{\bar{\omega}_c}{\omega_c} + \left\{1 - \frac{2\omega_p^2}{\omega(\omega-\bar{\omega}_c)}\frac{\bar{\omega}_c}{\omega_c} + \frac{\omega_p^4}{\omega^2(\omega-\bar{\omega}_c)^2}\frac{\bar{\omega}_c^2}{\omega_c^2}\right\}^{1/2}\right]$$

$$= \frac{\omega^2 \epsilon_L}{c^2}\left[-1 + \frac{\omega_p^2}{\omega(\omega-\bar{\omega}_c)}\frac{\bar{\omega}_c}{\omega_c}\right] \qquad (2.15a)$$

If we work within the restrictions outlined before , so that φ will be small , we can neglect the effect of attenuation. In what follows, we shall take $\beta \to 0$.

Using Eqs. (2.10b) and (2.11), we find

$$\frac{4\pi}{c}\vec{J} = -\frac{\omega_p^2}{c}\epsilon_L \frac{\omega}{\Delta}\frac{\bar{\omega}_c}{\omega_c} A_1\left[\hat{i}\cos(\xi-\chi-\varphi) + \hat{j}\sin(\xi-\chi-\varphi)\right] \qquad (2.16)$$

where the plasma frequency is defined by

$$\omega_p = \left(\frac{4\pi n e^2}{m^* \epsilon_L}\right)^{1/2} \qquad (2.17)$$

Introducing the dielectric function ϵ by

$$\nabla \times \vec{H} = \frac{4\pi}{c}\vec{J} + \frac{\epsilon_L}{c}\frac{\partial \vec{E}}{\partial t} = \frac{\epsilon}{c}\frac{\partial \vec{E}}{\partial t}$$

we find $$\frac{4\pi}{c}\vec{J} = \frac{\epsilon - \epsilon_L}{c}\omega^2 A_1\left[\hat{i}\cos(\xi-\chi) + \hat{j}\sin(\xi-\chi)\right]$$

Using the above equation with Eq. (2.16) and remembering the restriction of very small φ , we get the dielectric function as

$$\epsilon = \epsilon_L\left[1 - \frac{\omega_p^2}{\omega^2}\frac{\omega}{\Delta}\frac{\bar{\omega}_c}{\omega_c}\right] \qquad (2.18)$$

It is instructive to make a power series expansion of Eq. (2.18) in powers of the nonlinear parameter α . Taking $\zeta \to \infty$, we can approximate Δ by $(\omega - \bar{\omega}_c)$. Also to first order , Eq.(2.10d) can be rewritten as,

$$\bar{\omega}_c = \omega_c \left[1 - \frac{1}{2} \frac{v_0^2}{c^{*2}} \right]$$

Substituting for v_0 in the above equation from Eq. (2.10b) and using the result in Eq. (2.18), one obtains

$$\epsilon = \epsilon_L \left[1 - \frac{\omega_p^2}{\omega^2} \frac{\omega}{(\omega-\omega_c)-(\bar{\omega}_c-\omega_c)} \left\{ 1 - \frac{1}{2} \frac{\omega^2\alpha^2}{(\omega-\omega_c)^2} \right\} \right] + O(\alpha^4)$$

$$= \epsilon_L \left[1 - \frac{\omega_p^2}{\omega^2} \frac{\omega}{\omega-\omega_c} \left\{ 1 + \frac{\omega_c \left[-\frac{1}{2} \frac{\omega^2\alpha^2}{(\omega-\omega_c)^2} \right]}{\omega-\omega_c} \right\} \left\{ 1 - \frac{1}{2} \frac{\omega^2\alpha^2}{(\omega-\omega_c)^2} \right\} \right] + O(\alpha^4)$$

$$= \epsilon_L \left[1 - \frac{\omega_p^2}{\omega^2} \frac{1}{(1-\omega_c/\omega)} \left\{ 1 - \frac{1}{2} \frac{\alpha^2}{(1-\frac{\omega_c}{\omega})^2} - \frac{1}{2} \frac{\frac{\omega_c}{\omega}\alpha^2}{(1-\frac{\omega_c}{\omega})^3} + O(\alpha^4) \right\} \right]$$

$$= \epsilon_L \left[1 - \frac{\omega_p^2}{\omega^2} \frac{1}{(1-\omega_c/\omega)} \left\{ 1 - \frac{1}{2} \frac{\alpha^2}{(1-\frac{\omega_c}{\omega})^2} \left(1 + \frac{\omega_c/\omega}{(1-\omega_c/\omega)} \right) + O(\alpha^4) \right\} \right]$$

$$= \epsilon_L \left[1 - \frac{\omega_p^2}{\omega^2} \frac{1}{(1-\omega_c/\omega)} + \frac{\alpha^2}{2} \frac{\omega_p^2}{\omega^2} \frac{1}{(1-\omega_c/\omega)^4} + O(\alpha^4) \right]$$

(2.19)

We note the dramatic enhancement of the quadratic term as the magnetic field is made large enough so that ω_c approaches ω .

At first the fourth power enhancement of the quadratic term might appear surprising. But this is easily explained by considering the 'modulation' in the mass of the electron. To understand the origin of this modulation, we go back to the equation of motion Eq. (2.6). On examining thisequation, we find that the nonlinear effects result in modulating the electron mass from m^* to $m^*/(1 - v_o^2/c^2)^{1/2}$ which to first order is obtained by using Eqs. (2.10) as $m^* \left[1 + \frac{1}{2} \frac{\alpha^2}{(1-\omega_c/\omega)^2} \right]$

Now the linear dielectric function in the presence of a dc magnetic field is written as

$$\epsilon = \epsilon_L \left[1 - \frac{\omega_p^2/\omega^2}{1-\omega_c/\omega} \right] \tag{2.20}$$

To get the nonlinear dielectric function, remembering the mass dependence of ω_p and ω_c , and replacing the mass by the modulated mass, we get,

$$\epsilon = \epsilon_L \left[1 - \frac{\omega_p^2}{\omega^2 \left(1 + \frac{1}{2} \frac{\alpha^2}{(1-\omega_c/\omega)^2}\right)} \left\{ \frac{1}{1 - \frac{\omega_c}{\omega \left(1 + \frac{1}{2} \frac{\alpha^2}{(1-\omega_c/\omega)^2}\right)}} \right\} \right] \tag{2.21}$$

Expanding the above equation to quadratic terms in α ,

$$\epsilon = \epsilon_L \left[1 - \frac{\omega_p^2}{\omega^2} \left(1 - \frac{1}{2} \frac{\alpha^2}{(1-\omega_c/\omega)^2}\right) \left\{ \frac{1}{1 - \frac{\omega_c}{\omega}\left(1 - \frac{1}{2}\frac{\alpha^2}{(1-\omega_c/\omega)^2}\right)} \right\} \right]$$

$$= \epsilon_L \left[1 - \frac{\omega_p^2}{\omega^2} \left(1 - \frac{1}{2} \frac{\alpha^2}{(1-\omega_c/\omega)^2}\right) \frac{1}{(1-\frac{\omega_c}{\omega})} \left(1 - \frac{\alpha^2}{2} \frac{\omega_c/\omega}{(1-\omega_c/\omega)^3}\right) \right]$$

$$= \epsilon_L \left[1 - \frac{\omega_p^2}{\omega^2} \frac{1}{(1-\omega_c/\omega)} + \frac{\alpha^2}{2} \frac{\omega_p^2}{\omega^2} \frac{1}{(1-\omega_c/\omega)^4} + \mathcal{O}(\alpha^4) \right]$$

which is the same as Eq. (2.19) obtained before.

C. Self-Focusing Equations

The fact that the dielectric constant displays a nonlinear behavior has a profound influence on the propagation of electromagnetic waves through the medium. In a laser beam, in general, the intensity is not uniform along the profile of the beam, being maximum at the center and tapering off to zero along the edges. Therefore the nonlinearity of ϵ results in presenting different dielectric constants to different parts of the beam, thereby causing self-refraction. As long as the dielectric constant increases with increasing field, the result will be a refraction of the beam into the region where the intensity is greatest, thus giving the self-focusing effect. Since all beams in general possess fluctuations, self-focusing will occur even for 'uniform' beams.

In general there will be a competition between diffraction effects due to the confinement of the beam to a finite width, and a focusing effect due to the nonlinearity of the medium. The latter effect must dominate for self-focusing to occur. This will happen when the power exceeds some critical power.

A comprehensive review of electrodynamics of self-focusing has been presented by Akhmanov, Sukhorokov and Khokolov [33]. An alternative derivation of the self-focusing equations which proceeds directly from a variational principle has been developed by Tzoar and Gersten [28]. They

treat the self-focusing of a monochromatic linearly polarized wave. Here we apply their variational approach to derive the self-focusing equations for the case of a monochromatic circularly polarized wave. This approach has several benefits not enjoyed by the derivation of previous authors. Firstly, we have the computational advantage of having a variational principle. In principle this could be used computationally to optimize the trial focusing trajectories. Secondly, it provides us with a natural extension of Fermat's principle.

We start with the expression for the Lagrangian density for an electromagnetic wave interacting with a nonlinear dielectric :

$$\mathcal{L} = \epsilon_L (E^2 - B^2)/8\pi + \int \vec{P} \cdot d\vec{E} = \mathcal{L}_0 + \mathcal{L}_I \qquad (2.22)$$

where $\vec{P}$ is the polarization vector.

The variation principle is that

$$\delta \left(\frac{1}{\tau}\right) \int_0^\tau dt \int d\vec{r}\, \mathcal{L} = 0 \qquad (2.23)$$

where we assume that the end points $(0,\tau)$ are held fixed. In the free part of the Lagrangian, $\mathcal{L}_0$, we regard the fields as stemming from the vector potential $\vec{A}$, which for the circularly polarized wave, is of the form

$$\vec{A} = A\left[\hat{i}\cos(\omega t - kz - k\varsigma) + \hat{j}\sin(\omega t - kz - k\varsigma)\right]$$

$$\equiv A\left[\hat{i}\cos\delta + \hat{j}\sin\delta\right] \qquad (2.24)$$

where the amplitude A and the eikonal s are taken to be slowly varying functions of z . Since in self-focusing one finds rather narrow necks in the region of the focal length, we allow A and s to vary rapidly in the radial direction. A and s are time independent. Furthermore, azimuthal symmetry is assumed. The effect of the external magnetic field is completely buried in the dielectric function ϵ . We will work in the domain where the focal length is much smaller than the attenuation length $1/\beta$. Then the ohmic losses may be ignored to a first approximation and attenuation may be disregarded. The theory is therefore limited to the short distance propagation of the beam through the medium.

From Eq. (2.24) we obtain the electric and magnetic fields as

$$\vec{E} = -\frac{1}{c}\frac{\partial \vec{A}}{\partial t}$$

$$= E_0 \left[-\hat{i} \sin\delta + \hat{j} \cos\delta \right]$$

where $E_0 = kA$

and

$$\vec{B} = \nabla \times \vec{A}$$

$$= \hat{i} \left[E_0 \left(1 + \frac{\partial s}{\partial z}\right) \cos\delta - \frac{1}{k}\frac{\partial E_0}{\partial z} \sin\delta \right]$$

$$+ \hat{j} \left[E_0 \left(1 + \frac{\partial s}{\partial z}\right) \sin\delta + \frac{1}{k}\frac{\partial E_0}{\partial z} \cos\delta \right]$$

$$+ \hat{k} \left[\left(-E_0 \cos\theta \frac{\partial s}{\partial R} - \frac{1}{k} \sin\theta \frac{\partial E_0}{\partial R} \right) \cos\delta \right.$$

$$\left. + \left(-E_0 \sin\theta \frac{\partial s}{\partial R} + \frac{1}{k} \cos\theta \frac{\partial E_0}{\partial R} \right) \sin\delta \right]$$

where $x = R\cos\theta$ and $y = R\sin\theta$.

These give

$$E^2 = E_0^2 \tag{2.25a}$$

and

$$\begin{aligned} B^2 = {} & E_0^2 \left\{ 1 + 2\frac{\partial S}{\partial Z} + \left(\frac{\partial S}{\partial Z}\right)^2 \right\} + \frac{1}{K^2}\left(\frac{\partial E_0}{\partial Z}\right)^2 \\ & + E_0^2 \left(\frac{\partial S}{\partial R}\right)^2 \left(\cos^2\theta \cos^2\delta + \sin^2\theta \sin^2\delta \right) \\ & + \frac{1}{K^2}\left(\frac{\partial E_0}{\partial R}\right)^2 \left(\sin^2\theta \cos^2\delta + \cos^2\theta \sin^2\delta \right) \\ & + 2\frac{E_0}{K}\frac{\partial S}{\partial R}\frac{\partial E_0}{\partial R} \cos\theta \sin\theta \left(\cos^2\delta - \sin^2\delta \right) \\ & + 2\left(E_0 \cos\theta \frac{\partial S}{\partial R} + \frac{1}{K}\sin\theta \frac{\partial E_0}{\partial R} \right)\left(E_0 \sin\theta \frac{\partial S}{\partial R} - \frac{1}{K}\cos\theta \frac{\partial E_0}{\partial R} \right) \cos\delta \sin\delta \end{aligned} \tag{2.25b}$$

Now we substitute these values for E^2 and B^2 in the variational principle. The time integration of the action principle can be executed with the effect that $\cos^2\delta$ and $\sin^2\delta$ are replaced by their average values $1/2$, while the average value of $\cos\delta\sin\delta$ is zero.

In the integration of $\mathcal{L}_I$ we introduce the electric susceptibility χ by the equation

$$\vec{P} = \chi\left(E_0^2\right)\vec{E} \tag{2.26}$$

In the variational principle, the main variation of $\vec{P}.d\vec{E}$ is through the $\vec{E}$ part of $\vec{P}$, rather than the χ part. So we can replace $\int \vec{P}.d\vec{E}$ by $\chi(\overline{E_0^2}) \int \vec{E}.d\vec{E}$ where $\overline{E_0^2}$ is the average value of E_0^2.

Hence we obtain the variational principle as

$$\begin{aligned} \frac{\epsilon_L}{8\pi}\, \delta \int d\vec{r}\, \frac{1}{2} \Bigg[& -2E_0^2 \left\{ 2\frac{\partial S}{\partial Z} + \left(\frac{\partial S}{\partial Z}\right)^2 \right\} - \frac{2}{K^2}\left(\frac{\partial E_0}{\partial Z}\right)^2 - E_0^2\left(\frac{\partial S}{\partial R}\right)^2 \\ & - \frac{1}{K^2}\left(\frac{\partial E_0}{\partial R}\right)^2 + \frac{16\pi}{\epsilon_L}\chi\frac{E_0^2}{2} \Bigg] = 0 \end{aligned}$$

or

$$-\frac{\epsilon_L}{16\pi}\,\delta\int d\vec{r}\left[\frac{1}{\kappa^2}\left\{\left(\frac{\partial E_0}{\partial z}\right)^2+\frac{1}{2}\left(\frac{\partial E_0}{\partial R}\right)^2\right\}+E_0^2\left\{\left(\frac{\partial S}{\partial z}\right)^2+2\left(\frac{\partial S}{\partial z}\right)+\frac{1}{2}\left(\frac{\partial S}{\partial R}\right)^2\right\}-\frac{4\pi}{\epsilon_L}\chi E_0^2\right]=0 \tag{2.27}$$

Now we make the eikonal approximation and neglect the $\left(\frac{\partial E_0}{\partial z}\right)^2$ and $\left(\frac{\partial S}{\partial z}\right)^2$ terms. In analogy with the previous work on self-focusing, we express the amplitude and eikonal as :

$$E_0^2 = \left[E_i / f(z)\right]^2 \exp\left(-\frac{2R^2}{(af)^2}\right) \tag{2.28a}$$

$$S = \varphi(z) + R^2\beta(z)/2 \tag{2.28b}$$

Here E_i is the initial central field intensity, f(z) is the dimensionless radius of the beam and a is the initial beam radius. The variables φ, β and f are dependent on z . The boundary conditions are

$$\varphi(0) = \beta(0) = 0 \quad ; \quad f(0) = 1 \tag{2.29a}$$

and denoting the derivatives with respect to z by a prime,

$$\varphi'(0) = \beta'(0) = 0 \quad ; \quad f'(0) = 0 \tag{2.29b}$$

The average $\overline{E_0^2}$ is given by

$$\overline{E_0^2} = \frac{1}{2}E_i^2 \tag{2.30}$$

On examining Eq. (2.27) and performing the R integration, we see that z plays the role conventionally allotted to the time variable. The

quantities φ , β and f are now dynamical variables in the 'time' variable z . From Eqs. (2.28) we obtain,

$$\frac{\partial E_0}{\partial R} = -\frac{E_i}{f(z)} \frac{2R}{a^2 f^2} \exp\left(-\frac{R^2}{a^2 f^2}\right) \tag{2.31a}$$

$$\frac{\partial S}{\partial R} = R\beta(z) \tag{2.31b}$$

and

$$\frac{\partial S}{\partial z} = \varphi' + \tfrac{1}{2} R^2 \beta' \tag{2.31c}$$

Substituting Eqs. (2.31) in Eq. (2.27) and remembering the eikonal approximation, we obtain for the Lagrangian,

$$L = -\frac{\epsilon_L}{8} \int_0^\infty R\, dR \left[\frac{2}{k^2} \frac{E_i^2 R^2}{a^4 f^6} \exp\left(-\frac{2R^2}{a^2 f^2}\right) + \frac{E_i^2}{2f^2} \beta^2 R^2 \exp\left(-\frac{2R^2}{a^2 f^2}\right) + 2\frac{E_i^2}{f^2}\left(\varphi' + \tfrac{1}{2} R^2 \beta'\right) \exp\left(-\frac{2R^2}{a^2 f^2}\right) - \frac{4\pi\chi}{\epsilon_L} \frac{E_i^2}{f^2} \exp\left(-\frac{2R^2}{a^2 f^2}\right) \right]$$

Performing the R integration we obtain,

$$L = -\frac{\epsilon_L E_i^2 a^2}{32} \left[2\varphi' - \frac{4\pi\chi}{\epsilon_L} + \frac{1}{k^2 a^2 f^2} + \frac{\beta^2 a^2 f^2}{4} + \frac{\beta' a^2 f^2}{2} \right] \tag{2.32}$$

The term φ' , being an exact differential is superfluous and can be dropped. The Hamiltonian corresponding to the above Lagrangian is given by

$$H = \frac{\epsilon_L E_i^2 a^2}{32} \left[\frac{1}{(afk)^2} + \left(\frac{\beta a f}{2}\right)^2 - \frac{4\pi\chi}{\epsilon_L} \right]$$

From the equation of motion for the above Hamiltonian we obtain $\beta = 2f'/f$ so that

$$H = \frac{\epsilon_L E_i^2 a^2}{32}\left[\frac{1}{(afk)^2} + (af')^2 - \frac{\epsilon-\epsilon_L}{\epsilon_L}\right] \tag{2.33}$$

where we have used the fact that $\epsilon = \epsilon_L + 4\pi\chi$. We must remember that in the above, ϵ is a function of the average intensity $\frac{1}{2}E_0^2$.

Eq. (2.33) can be given a simple mechanical analogue. Let

$$m = \frac{\epsilon_L E_i^2 a^4}{16} \tag{2.34a}$$

$$L = \frac{\epsilon_L E_i^2 a^2}{16k} \tag{2.34b}$$

$$V = \frac{E_i^2 a^2}{32}(\epsilon_L - \epsilon) \tag{2.34c}$$

Then Eq. (2.33) becomes

$$H = \frac{m}{2}\left(\frac{df}{dz}\right)^2 + \frac{L^2}{2mf^2} + V \tag{2.35}$$

which is the Hamiltonian for a particle of mass m and angular momentum L moving in a potential V. Thus all the familiar notions regarding motion of a particle bound in a potential field can be transferred directly to the self focusing problem. In particular, the concept of effective potential[40] can be quite usefully employed. Thus we define

$$V_{eff} = V + L^2/2mf^2 \tag{2.36}$$

If V_{eff} has an absolute minimum, then we have the possibility of self-focusing. This corresponds to the mechanical analogue of having a bound noncircular orbit. At the minimum of V_{eff}, we would have self trapping which is analogous to circular orbits.

The main concern of the self-focusing effect is the variation of f with z, and the condition for self-focusing is that V_{eff} have a minima for $0 \lesssim f \lesssim 1$. When self focusing does occur, the focal length is given by the distance required to go from maximum to minimum radius. Since our initial radius f is 1, and denoting the minimum radius by F, we get the focal length as

$$Z_F = \int_1^F \frac{df}{\left[\frac{2}{m}(H - V_{eff})\right]^{1/2}} \tag{2.37}$$

Using the expression derived for ϵ in Eq. (2.18) the effective potential for motion in the 'f' direction can be written as

$$V_{eff} = \frac{\epsilon_L E_i^2 a^2}{32}\left[\frac{1}{(afk)^2} + \frac{\omega_p^2}{\omega^2}\frac{\omega}{\Delta}\frac{\bar{\omega}_c}{\omega_c}\right] \tag{2.38}$$

We note that $\bar{\omega}_c$ and Δ depend on power which is now defined through

$$\alpha^2(\bar{E}_0^2) = \frac{E_i^2}{2f^2}\left(\frac{e}{m^* c^* \omega}\right)^2 \equiv \frac{\gamma}{f^2} \tag{2.39}$$

An inspection of the expression for V_{eff} shows that as f decreases, the first term increases while the second term decreases. Eventually at small f the first term completely dominates. This is the region where diffraction effects are very important. At larger f the refraction effects, represented by the second term in Eq. (2.38) become more important. The beam starts out initially with beam radius $f = 1$ at $z = 0$. If a minimum in V_{eff} exists in the region $0 \lesssim f \lesssim 1$, then focusing will occur. The condition that there exist a minimum will correspond to the existence of a critical power P_{cr} for self-focusing to occur. It is clear from Eq.(2.38) that the critical power will now be dependent on the magnetic field in some non-trivial fashion.

Before going on to discuss the numerical computation of the various quantities it will be helpful to derive an analytical formula for the low field limit. Thus we utilize the low field result for the nonlinear dielectric function, derived in Eq. (2.19) and write the effective potential as,

$$V_{eff} = \frac{\epsilon_L E_i^2 a^2}{32}\left[\frac{\omega_p^2/\omega^2}{1-\omega_c/\omega} + \frac{1}{(afK)^2} - \frac{\alpha^2}{2}\frac{\omega_p^2}{\omega^2}\left(\frac{1}{1-\omega_c/\omega}\right)^4\right] \tag{2.40}$$

The chief drawback of this approximation is that it predicts that the beam radius will shrink to zero when self-focusing occurs. In reality

the higher order terms in α cause a saturation effect which, when combined with the diffraction effect, limits the ultimate beam radius. Still, the Eq. (2.40) is useful to make an estimate of the enhancement of the nonlinear effect by the magnetic field. Defining the critical central field intensity E_i^{cr} as the intensity when the last two terms in Eq. (2.40) are equal, and using Eq. (2.39) we predict a critical power corresponding to a central field intensity

$$E_i^{cr} = \frac{\sqrt{2}\, m^* c^* \omega^2}{e\alpha k \omega_p} \left(1 - \omega_c/\omega\right)^2$$

We therefore expect a marked deviation of the critical power from what it would be in the absence of the magnetic field, varying roughly as the fourth power of $(1 - \omega_c/\omega)$. Consequently, we expect to find that the critical power can be depressed by several orders of magnitude without much difficulty.

D. Results and Discussion

In the previous sections we derived an expression for the nonlinear dielectric constant for a semiconductor in a dc magnetic field. We found that a substantial enhancement of the nonlinear behaviour is possible when the cyclotron frequency is close to the frequency of the incident radiation. This enhancement, coupled with the fact that even without a magnetic field the nonlinear behaviour is strong, produces the largest nonlinear dielectric behaviour known.

The mechanism for the enhancement is simple. In the absence of a magnetic field, the electrons are constantly accelarated to some peak velocity given by $e\vec{E}/m^*\omega$ where $\vec{E}$ is the electric field. The electrons are then decelerated untill they reach this speed in the opposite direction. This process repeates itself periodically. Since the nonlinearity is essentially a quasi relativistic effect , a measure of the nonlinearity of the system is provided by $eE/m^*\omega c^* = \alpha$. In the presence of a magnetic field the electrons are moving along the cyclotron orbits. As the velocity of the electrons is bent in the opposite direction by the magnetic field, the polarization vector of the incident light is also pointing in the opposite dipection. Thus the light can coherently accelarate the electrons for many cycles. In the steady state , the electron is driven at the frequency of the incident radiation and its velocity is finally 90^o out of phase with electrical force , so that the field stops doing work on the electrons.

The peak velocity is largely enhanced however. The chief limitation on the electron accelaration is the collision time τ . For this reason, we never allowed ω_c to approach too closely to ω .

Using the expression and formalism derived in previous sections , we now obtain results for a case of practical interest. Our calculations are done for the semiconductor InSb , which is chosen for several[41] reasons. It has a low electronic effective mass $m^* = m_e / 60$ where m_e is the free electron mass , and relatively small gap energy $E_g = 0.234$ eV. This yields $c^* = 1.11 \times 10^8$ cm/sec which is $1 / 270$ the velocity of light. This validates the approximation $c^*/c \ll 1$ made before. Here ϵ_L was taken to be 16.

The radiation frequency was taken to correspond to the CO_2 laser, $\omega = 1.742 \times 10^{14}$ rad/sec. The plasma frequency was chosen to be such that $\omega_p^2 = \omega^2/10^3$ corresponding to a carrier concentration of $n = 2.55 \times 10^{15}$ cm^{-3}. Under these conditions, the free carrier absorption is very small, especially if the experiment is performed around liquid nitrogen temperature ($T = 77^{\circ}$ K). For this frequency ω , two photon absorption is energetically forbidden and therefore it is easy to transmit the radiation through the crystal. Also since $\omega \gg \omega_p$, one may neglect cooperative plasma effects. For these parameters the cold dilute plasma approximation is well justified. In our calculations, we will never let the cyclotron frequency ω_c exceed 0.8ω. This value is away from resonance and corresponds to a magnetic field of 132 KGauss , a value obtainable

in the laboratory.

In Fig. 1 we present the dielectric constant ϵ as a function of the dimensionless power parameter $\gamma = \frac{1}{2}(eE_i/m^*c^*\omega)^2$ for several values of the cyclotron frequency ω_c. Comparing the curves for which $\omega_c = 0.8\,\omega$ and $\omega_c = 0.3\,\omega$ with the curve for which $\omega_c = 0$, we note the large effect of the magnetic field on the nonlinearity of the dielectric constant. This is readily explained by the factor $(1-\omega_c/\omega)^{-4}$ in Eq.(2.19) The numerical results plotted in Fig. 1 also display the saturation of ϵ when γ becomes large.

We now employ this dielectric constant in calculating the self-focusing of the beam. In Fig. 2, the effective potential V_{eff} of Eq.(2.38) is plotted as a function of the dimensionless beam radius f. The repulsive part of the potential represents the diffraction effect while the attractive part is due to refraction. The initial beam radius was taken to be 0.0054 cm, corresponding to five vacuum wavelengths. The potential curves are presented for several values of ω_c/ω and several values of γ. Exploiting the analogue with centralforce motion, wecan think of the 'time' that it takes for a particle to go from $f = 1$ to the other intersection with the V_{eff} curve as the self-focusing distance. The focal spot radius F corresponds to the value of f at this intersection, i.e.

$$V_{eff}\Big|_{f=1} = V_{eff}\Big|_{f=F}$$

For those curves in which the magnetic field is absent, we find

that the beam shrinks to roughly $F = 0.4$. On the other hand for large magnetic field like for $\omega_c = 0.8\,\omega$, f shrinks to about $F = 0.2$. Along with this five fold shrinkage in beam radius is associated a twenty five fold increase in central beam intensity. The relative insensitivity of the minimum beam radius to power or magnetic field points to the fact that it is essentially determined by diffractive rather than refractive effects.

The critical power can be found by plotting the effective potential curves for decreasing values of γ . At critical power the V_{eff} vs f curve just stops having a minimum. We find that, for example, for $\omega_c = 0.8\,\omega$ and $\gamma = 0.0003$ self-focusing is still possible. This corresponds to an input power of only eight watts. The beam focuses to a radius of $F = 0.329$ in a focal length of $224a = 12.1$ mm. The critical power lies just slightly below eight watts, where the focal length becomes infinite.

The beam radius as a function of the propagation distance is presented in Fig. 3 for several values of γ at $\omega_c/\omega = 0.8$. As one might expect, an increase in γ leads to a more precipitous focusing and hence a shorter focal length. For comparison's sake we illustrate in Fig. 4 a similar set of curves for the case of no magnetic field. We note that much larger power is required to obtain the same focal lengths than when the magnetic field is present. In each case, after focusing to the minimum radius F , the beam will bounce back to reach its initial width. The process will continue periodically with a period $2z_F$. The figures only show one half of the period as the curves are symmetrical about the turning

point. Here the attenuation of the beam as it travels in the semi-conductor has been neglected. The effect of attenuation is to cause z_F to change as a function of z and ultimately to become infinite. It is worthwhile comparing the with field case with the no field case. Without the B-field, to obtain a focal length $z_F = 6$ mm requires $\gamma = 1.0$. From Fig. 5, (see below), we see that in the presence of the B field the same focal length is obtained with $\gamma = 0.0006$.

In the above calculations, the attenuation of the beam, as it passes through the semi-conductor has been neglected. Thus we limit ourselves to the case of long photon meanfree path. To justify this procedure, we compute some values for the attenuation length. This is done by using Eq. (2.15) for β^2 obtained earlier. It is to be noted that β is a function of the power γ .As the beam is focused, the power along the beam changes because of the change in f , thus giving variation to values of β along the beam. At the initial stages of contraction of the beam, a rather large β value is obtained, but as the beam contracts in radius, this value is rapidly depressed. By 'averaging' β over f from $f = 1$ to $f = F$, the focal spot radius, and then calculating β^{-1} , we can get a reasonable estimate for the attenuation length. The attenuation length is thus computed and plotted as a function of the power γ in Fig. 5. For comparison, the focal length z_F is also plotted on the same graph. As the attenuation length is found to be strongly dependent on the carrier density n , the results are obtained for $n = 2.55 \times 10^{15}$ cm^{-3} used so

far in the calculations and also for a larger value $n = 6.4 \times 10^{15}$ cm^{-3}. It is seen that for the first case, for large values of γ, the attenuation length is at least one order of magnitude larger than z_F while even for small γ, $\beta^{-1} >> z_F$, thus justifying the neglect of attenuation in our calculations for z_F. For the larger n, the results for z_F are really valid only for large γ values where $\beta^{-1} >> z_F$. Thus the increased effect of attenuation of the beam precludes the possibility of obtaining magnetic field enhancement of self-focusing in samples with $n \gtrsim 2 \times 10^{16}$ cm^{-3}, for InSb samples.

Fig. 5 also shows that there is a marked decrease in z_F with γ only for small γ. For large γ, there is practically no variation at all. This corresponds to the fact that nonlinear dielectric constant ϵ saturates for large γ. This can also be understood by examining the effective potential curves in Fig. 2. One notes that for a strong magnetic field (e.g. $\omega_c/\omega = 0.8$), the main effect of increasing the power γ is to vertically displace the potential curve. Since the focusing length is analogous to the time required to go from a maximum orbit radius to a minimum orbit radius, and this is unaffected by a vertical translation of the potential curve, we can understand the insensitivity of z_F with γ. The only reason that we have to work with moderate powers instead of weak powers is to overcome the attenuation effects. In fact at very large powers, we even detect a small increase in z_F with increasing intensity.

Here we have shown that there is a resonant enhancement of the

self-focusing effect. This resonance occurs between ω and $\bar{\omega}_c$. The chief manifestation of this resonance is observed in Figs. 3 and 4 where one sees a sharp initial variation of beam radius with propagation distance when the magnetic field is present. It should be noted that $\bar{\omega}_c$ is power dependent and consequently a detuning from resonance can occur if the strength of the beam gets considerable, as when the beam focuses. This is the reason for the initial sharp variation of the beam radius with propagation distance, followed by relatively slow variation as the central beam intensity increases near the focus. In Fig. 5 , the small increase in z_F with power, at very large power is also a result of the considerable detuning from resonance.

Finally, in Fig. 6, we present $\bar{\omega}_c/\omega$ as a function of ω_c/ω for various values of the power parameter γ . At small intensities, the two quantities are essentially the same, as expected. At large γ , however, there is a considerable shift.

CHAPTER III

Consequences of Self-Induced Transparency in Semiconductors

A. Indroduction

It has been recognized for some time that the propagation of electromagnetic pulses in a medium is radically different at low and high electric field intensities. Self-induced transparency is the phenomenon in which a high intensity electromagnetic pulse is able to be transmitted through a medium which is opaque at low pulse intensities. It has been the object of considerable study in recent years for both atomic and solid-state systems[9,10,42]. Two types of self-induced transparencies have been identified - absorptive and dispersive. For the case of an absorptive[9,10,42] system, at weak pulse intensities, the pulse is attenuated in the usual Beer's law manner. At higher intensities, however, it is possible for the leading edge of a pulse to be absorbed and have its trailing edge stimulate reemission , thereby feeding the energy back to the pulse and thus resulting in self-induced transparency.

In dispersive systems, on the other hand, the opacity of the medium is due to a frequency cutoff at the plasma frequency. An inspection of the dispersion relation $k^2c^2 = \epsilon_L(\omega^2 - \omega_p^2)$, where ϵ_L is the dielectric function of the background, shows that when the carrier frequency ω approaches the plasma frequency from above, the wave vector k approaches

zero. For carrier frequencies below the plasma frequency, k is imaginary and thus the medium becomes opaque. If the dispersive properties of the medium are altered by an intense field , then what once was opaque may become transparent. Soliton propagation may occur due to the balance of dispersive and nonlinear effects, the former tending to expand the pulse and the latter tending to compress it.

An example of a system where this phenomenon can occur is the narrow gap semiconductor, where the change in the dispersive properties of the medium takes place due to the nonlinearity associated with the nonparabolicity of the conduction band. Another system is the gaseous[43] plasma where relativistic effects generate the desired nonlinearity. In this chapter we consider the case of narrow gap semiconductors and discuss some consequences of self-induced transparency.

Self-induced transparency in narrow gap semiconductors has been studied by Tzoar and Gersten[44] . They demonstrated the existence of soliton-like pulse solutions to such systems and showed that nonlinear propagation for frequencies below the plasma frequency of the system is possible provided we keep a certain relation between the duration of the pulse and its total energy. Analytical expressions for such pulse-like propagation are obtained in section B.

One consequence of self-induced transparency is the modification

in the reflectivity properties of the semiconductor. In the linear optics domain, one generally regards the reflectivity as a function of frequency but independent of intensity. In particular, one thinks of the plasma frequency cutoff as invariant under intensity changes. However nonlinear effects result in plasma frequency being intensity dependent in narrow-gap semiconductors. In section C , we explore the reflectivity curve's dependence on intensity.

In addition to the problem of steady-state pulse propagation, one can ask for an analysis of some boundary value problems or initial condition problems. In section D, we consider numerical solutions to such problems as pulse reflection/transmission at a boundary, pulse transmission through a slab and the effect of attenuation due to collisions on pulse propagation through a nonlinear medium.

B. Self Induced Transparency

It is well known that for weak intensities it is not possible for electromagnetic radiation to propagate in a crystal for frequencies below the plasma frequency. At higher intensities however, nonlinear effects become important and propagation might be possible. In narrow gap-semiconductors, the nonlinear effects due to nonparabolic bands result in a velocity dependent mass for the electron. A strong electromagnetic field then imparts to the conduction electrons an appreciable mean square velocity, thereby enhancing the average effective mass. As the plasma frequency decreases monotonically with increasing mass it can be depressed below the incident radiation frequency. When the local plasma frequency in the vicinity of the pulse is depressed sufficiently, propagation can occur. Thus the propagation is induced by the strong pulse itself. A detailed study of self-induced transparency in semiconductors can lead to an improved understanding of the nonlinear optical properties of such crystals.

Here we follow the treatment given by Tzoar and Gersten[44] to derive the self-induced transparency equations in semiconductors. We begin by considering the nonlinear propagation of a plane electromagnetic wave in a narrow-band-gap semiconductor like InSb. The wave is characterized by its vector potential $\vec{A}$. Following Kane[39], the dynamics of an electron at the bottom of the conduction band is

governed in the presence of the electromagnetic wave, by the Hamiltonian,

$$H = \left[(m^* c^{*2})^2 + \left(\frac{eAc^*}{c} \right)^2 \right]^{1/2} \tag{3.1}$$

Here m^* is the effective mass of the conduction electron and the parameter c^* is related to the energy gap E_g through $c^* = (E_g / 2m^*)^{1/2}$. As for the electron dynamics, c^* plays the same role as the conventional speed of light c. In semiconductors, where c^* can be smaller than c by as much as two orders of magnitude, the relativistic nonlinearities are much stronger than in gaseous plasmas.

From Eq. (3.1), using Hamilton's equations of motion, the induced current density is given by

$$\vec{J} = -nc \frac{\partial H}{\partial \vec{A}}$$

$$= -\left[1 + \left(\frac{eA}{m^* c^* c} \right)^2 \right]^{-\frac{1}{2}} \frac{ne^2 \vec{A}}{m^* c} \tag{3.2}$$

where n is the carrier concentration.

Substituting this value of $\vec{J}$ in the wave equation

$$\nabla^2 \vec{A} - \frac{\epsilon_L}{c^2} \frac{\partial^2 \vec{A}}{\partial t^2} = -\frac{4\pi}{c} \vec{J} \tag{3.3}$$

one obtains the nonlinear equation for $\vec{A}$ as,

$$\nabla^2 \vec{A} - \frac{\epsilon_L}{c^2} \frac{\partial^2 \vec{A}}{\partial t^2} = \frac{\epsilon_L}{c^2} \omega_p^2 \vec{A} \left[1 + \left(\frac{eA}{m^* c^* c} \right)^2 \right]^{-\frac{1}{2}} \tag{3.4}$$

Here ϵ_L is the lattice dielectric constant and the plasma frequency is given by $\omega_p = (4\pi ne^2 / m^* \epsilon_L)^{1/2}$.

Considering the incident electromagnetic wave to be circularly polarized and propagating in the z-direction with wave vector k and frequency ω, we take,

$$\frac{e\vec{A}}{m^* c^* c} = \alpha \left[\hat{i} \cos(kz - \omega t - \chi) + \hat{j} \sin(kz - \omega t - \chi) \right] \tag{3.5}$$

As we are interested in the situation where the phase velocity has attained a steady state, the phase factor χ is taken to be a constant.

On substuting Eq.(3.5) in Eq.(3.4) and separating $\hat{i}$ and $\hat{j}$ components, one obtains the set of equations :

$$k \frac{\partial \alpha}{\partial z} + \frac{\omega \epsilon_L}{c^2} \frac{\partial \alpha}{\partial t} = 0 \tag{3.6}$$

$$\frac{\partial^2 \alpha}{\partial z^2} - \frac{\epsilon_L}{c^2} \frac{\partial^2 \alpha}{\partial t^2} - \alpha \left(k^2 - \frac{\epsilon_L}{c^2} \omega^2 \right) = \frac{\epsilon_L}{c^2} \omega_p^2 \frac{\alpha}{(1+\alpha^2)^{1/2}} \tag{3.7}$$

Integration of Eq. (3.6) implies that α is an arbitrary function of $\xi = \frac{\omega z}{c} \epsilon_L^{1/2} - \frac{kc}{\epsilon_L^{1/2}} t$.

Thus the group velocity is simply $kc^2/\omega\epsilon_L$. On substituting this functional form of α as a function of ξ in Eq. (3.7), one obtains,

$$\frac{d^2\alpha}{d\xi^2} + \alpha = \frac{\omega_p^2}{\omega^2 - \frac{k^2 c^2}{\epsilon_L}} \frac{\alpha}{(1+\alpha^2)^{1/2}} \tag{3.8}$$

The first integral of this equation, with the initial condition $\frac{d\alpha}{d\xi} = 0$ when $\alpha = 0$, gives,

$$\left(\frac{d\alpha}{d\xi}\right)^2 = -\alpha^2 + \frac{2\omega_p^2}{\omega^2 - \frac{k^2c^2}{\epsilon_L}}\left[(1+\alpha^2)^{1/2} - 1\right] \tag{3.9}$$

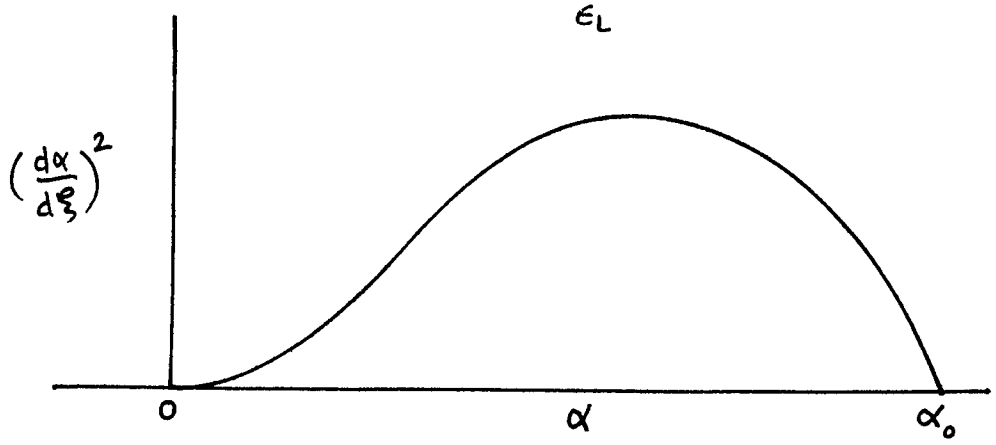

When $\left(\frac{d\alpha}{d\xi}\right)^2$ from Eq. (3.9) is plotted as a function of α, one finds that $\left(\frac{d\alpha}{d\xi}\right)^2$ again becomes zero at the value α_0 where

$$(1+\alpha_0^2)^{1/2} = \frac{2\omega_p^2}{\omega^2 - k^2c^2/\epsilon_L} - 1 \tag{3.10}$$

Since $\left(\frac{d\alpha}{d\xi}\right)$ starts at zero, one concludes that in an infinite amount of time, α increases from a value zero to its maximumvalue α_0 and then again bounces back to value zero.

To integrate Eq.(3.9) further, let $u = (1+\alpha^2)^{1/2}$ and $u_0 = (1+\alpha_0^2)^{1/2}$. This gives,

$$\left(\frac{du}{d\xi}\right)^2 = \frac{u^2-1}{u^2}\left[1 - u^2 + (u_0+1)(u-1)\right] \tag{3.11}$$

Taking $\xi = 0$ when $u = u_0$, Eq.(3.11) can be rewritten in the integral form,

$$\xi = \int_u^{u_0} \frac{u\,du}{(u-1)\left[(u+1)(u_0-1)\right]^{1/2}}$$

This integration can be done exactly to get the result,

$$\xi = \frac{\pi}{2} + \sin^{-1}\left(\frac{u_0 - 2u - 1}{u_0 + 1}\right) + \left[2(u_0-1)\right]^{-\frac{1}{2}} \ln\left[\frac{u(u_0-3) + 3u_0 - 1 + 2\left[2(u_0-1)(u_0-u)(u+1)\right]^{1/2}}{(u-1)(u_0+1)}\right] \tag{3.12}$$

For small α_0, ξ can be expanded in powers of α and α_0, and yields the pulse shape,

$$\alpha = \alpha_0 \operatorname{sech}\left(\tfrac{1}{2}\alpha_0 \xi\right) \tag{3.13}$$

We find the same characteristic hyperbolic secant pulse profile as is found in conventional self induced transparency as well as in other nonlinear propagation investigations[9,45]. In conventional self induced transparency, the concept of a 2π pulse is illuminating. A 2π pulse makes the medium 'transparent' to it and propagates without any attenuation in shape or size. Here the analogue of that concept can be found by performing the integral $\int_{-\infty}^{+\infty} \alpha \, d\xi$ which is indeed 2π. Thus the area under the pulse is a constant of motion independent of the amplitude.

In order to determine the amplitude α_0, we relate it to the energy per unit area of the pulse, W, where

$$W = \frac{\omega}{4\pi} \frac{\sqrt{\epsilon_L}}{c} \left(\frac{m^* c^* c}{e}\right)^2 U \tag{3.14a}$$

$$U = \int_{-\infty}^{+\infty} \alpha^2 \, d\xi = 4\alpha_0 \tag{3.14b}$$

The dispersion relation is given by

$$\omega^2 = \frac{K^2 c^2}{\epsilon_L} + 2\omega_p^2 \left[1 + (1 + U^2/16)^{1/2} \right]^{-1} \qquad (3.15)$$

As $U \to 0$, this reduces to the standard dispersion relation $\omega^2 = K^2c^2/\epsilon_L + \omega_p^2$. Thus we observe a depression of the cut-off frequency below ω_p .

In the conventional self-induced transparency one is concerned with an absorptive system. The pulse solution is the case where the leading edge of the pulse is absorbed and the trailing edge stimulates subsequent emission. In the present case, we are concerned with a dispersive system. A simple analogy can be made with the case of a transmission line. We imagine a distributed inductance existing along the line as shown below.

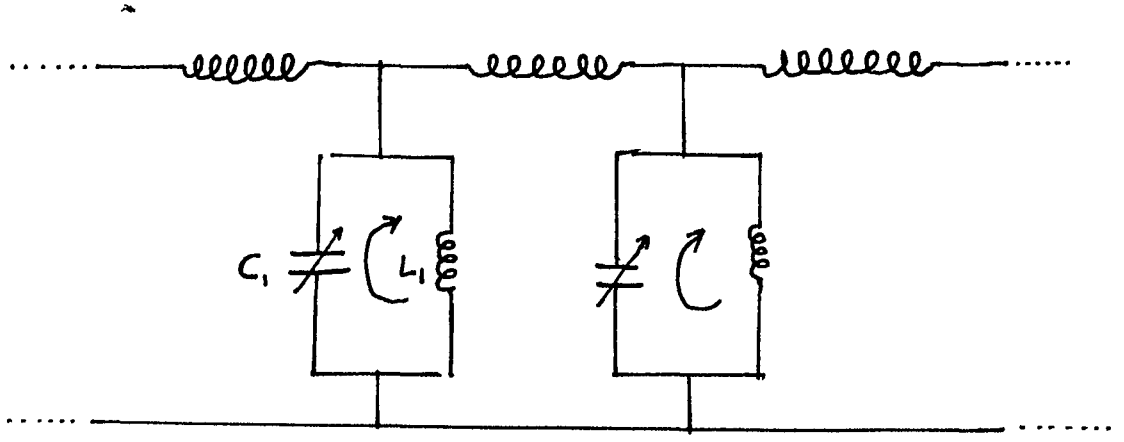

At regular intervals the line is shunted by resonant tank circuits whose characteristic frequency $\omega_p(V)$ depends on the voltage V . The tank's inductance (corresponding to electronic inertia) becomes appreciably larger as the voltage drop across it increases. For frequencies below ω_p and weak signals , the tank behaves like an inductor and no propagation is possible. At higher intensities however, the capacitance dominates and propagation will occur. The 2π pulse signifies the complete return of energy from the tank circuit to the transmission line.

In real solids, several limitations exist to the theory as presented here. Impurities would introduce dephasing collisions which might destroy the coherence of the pulse. Collision effects may be introduced phenomenologically by assigning an effective conductivity to the medium . This would introduce an ohmic energy loss into the propagation which would cause the energy of the pulse to decay exponentially. Since it remains a 2π pulse, the effect would be to broaden it and reduce its central amplitude.These nonlinear pulse propagations are numerically studied in section D.

C. Intensity Dependent Reflection

The reflection of light from solid surfaces is a well understood phenomenon as long as the light's intensity is weak. For light frequencies above the plasma frequency of the solid, the material is generally transparent while below the plasma frequency it is opaque. Thus the reflection efficiency, plotted as a function of light frequency displays a rather abrupt downward step as the plasma frequency is exceeded. The sharpness of this step is governed by the absorptive character of the material. A higher absorption coefficient results in a smoother downward step. The important thing to emphasize is that the reflection curve is generally regarded as independent of light intensity.

As the light intensity is elevated the situation becomes more complex due to nonlinear optical effects. The basic question we wish to consider here is whether or not the reflection curve depends on the light intensity. In particular, we focus our attention on the narrow band-gap semiconductors where the plasma frequency is determined by the level of the n-type doping. For the narrow-gap semiconductor, the energy momentum relation relation for the electrons is nonparabolic and the electrons acquire a velocity dependent mass . Modulation of the electronic velocity by the strong electromagnetic field induces an intensity dependent mass. An increased mass results in a depressed plasma frequency. Thus the location of the break in the reflection curve can be expected to be intensity dependent.

In order to obtain a qualitative appreciation for the effect, consider the following situation. A beam of monochromatic linearly polarized light is normally incident on a narrow band-gap semiconductor like InSb which is taken to occupy the space $z \geq 0$. Thus in vacuum one has both reflected and incident waves while in the crystal there is a transmitted wave. The crystal is characterized by a complex dielectric function of the form

$$\epsilon = \epsilon_1 + i \frac{4\pi\sigma}{\omega} \tag{3.16}$$

where σ is the conductivity of the solid and ω is the frequency of light. Here ϵ_1 is the real part of the dielctric function. A microscopic model will be employed to determine ϵ. The spatial dependence of the electric field in the skin depth region is neglected since the linear skin depth is much larger than the electron mean free path.

The reflection coefficient can be expressed in terms of ϵ in the standard manner as

$$R = \left| \frac{\epsilon^{1/2} - 1}{\epsilon^{1/2} + 1} \right| \tag{3.17}$$

We now obtain an expression for ϵ as a function of the field intensity. The equation of motion of an electron responding to the monochromatic linearly polarized electric field $\vec{E} \cos \omega t$ is

$$\frac{d\vec{p}}{dt} + \frac{\vec{p}}{\tau} = -e\vec{E} \cos \omega t \tag{3.18}$$

where $\vec{p}$ is the electronic momentum, $-e$ is the electronic charge and τ is a phenomenological relaxation time to account for the effect of electronic collisions. We neglect the effect of the ac magnetic force

since typical electronic speeds are much less than the speed of light.

The steady state solution to Eq. (3.18) is

$$\vec{p} = \vec{p}_0 \sin(\omega t + \psi) \tag{3.19a}$$

where

$$\vec{p}_0 = -\frac{e\vec{E}}{\omega}\left(1 + \frac{1}{\omega^2\tau^2}\right)^{-\frac{1}{2}} \tag{3.19b}$$

and

$$\psi = \tan^{-1}\left(\frac{1}{\omega\tau}\right) \tag{3.19c}$$

The single particle Hamiltonian for narrow-gap semiconductors formally resembles that of a relativistic electron provided the speed of light is replaced by

$$c^* = \left(\frac{E_g}{2m^*}\right)^{1/2} \tag{3.20}$$

where E_g is the band gap energy and m^* is the effective electron mass near the bottom of the conduction band[39]. Consequently the velocity is related to the momentum through the equation

$$\vec{v} = c^* \vec{p}\left[p^2 + (m^* c^*)^2\right]^{-1/2} \tag{3.21}$$

Insertion of Eq.(3.19) into Eq. (3.21) leads to an expression containing odd harmonics of ω :

$$\vec{v} = \frac{c^* \vec{p}_0 \sin(\omega t + \psi)}{\left[p_0^2 \sin^2(\omega t + \psi) + (m^* c^*)^2\right]^{1/2}}$$

$$= \sum_n V_n \sin\left[(2n+1)(\omega t + \psi)\right] \tag{3.22}$$

In the present discussion we are only interested in the fundamental harmonic so we neglect the higher order terms. Thus we project this harmonic and find

$$\vec{V}_0 = \frac{2}{\pi} \int_0^{\pi} \frac{c^* \vec{p}_0 \sin^2 \xi}{\left[p_0^2 \sin^2 \xi + (m^* c^*)^2 \right]^{1/2}} d\xi \qquad (3.23)$$

Using the integral[46]

$$\int_0^{2\pi} \frac{\sin^{2K+2} \xi \, d\xi}{\left[1 - \delta \cos^2 \xi\right]^{1/2}} = \frac{2\sqrt{\pi}\, \Gamma(K + \frac{3}{2})}{(K+1)!} F\left(\tfrac{1}{2}, \tfrac{1}{2}; K+2; \delta\right)$$

Eq. (3.23) reduces to

$$\vec{V}_0 = \frac{-e\vec{E}}{m^* \omega \left(1 + \frac{1}{\omega^2 \tau^2}\right)^{1/2}} \frac{1}{(1+\gamma)^{1/2}} F\left(\tfrac{1}{2}, \tfrac{1}{2}; 2; \frac{\gamma}{1+\gamma}\right) \qquad (3.24)$$

where F is the Gauss hypergeometric function and γ is a dimensionless parameter measuring the intensity of the field :

$$\gamma = \left(\frac{eE}{m^* c^* \omega}\right)^2 \frac{1}{1 + \frac{1}{\omega^2 \tau^2}} \qquad (3.25)$$

One may think of γ as essentially the square of the ratio of the ac velocity of the electrons to the characteristic speed c^*. It is thus a measure of the degree of relativistic behaviour to be expected, or alternately the degree of nonlinear behaviour in the problem.

The current density $\vec{J} = -ne\vec{v}$ is thus obtained as,

$$\vec{J} = \frac{ne^2\vec{E}}{m^*\omega}\,\frac{1}{\left(1+\frac{1}{\omega^2\tau^2}\right)^{1/2}}\,\frac{1}{(1+\gamma)^{1/2}}\,F\left(\tfrac{1}{2},\tfrac{1}{2};2;\frac{\gamma}{1+\gamma}\right)\sin(\omega t+\psi) \tag{3.26}$$

where n is the carrier density.

Using Maxwell's equations, $\vec{J}$ can also be obtained in terms of conductivity as,

$$\vec{J} = \sigma\vec{E}\cos\omega t - \frac{\epsilon_1-\epsilon_L}{4\pi}\,\omega\vec{E}\,\sin\omega t \tag{3.27}$$

where ϵ_L is the lattice dielectric constant.

A comparison of the two expressions for $\vec{J}$ provides us with the desired equations for σ and ϵ_1:

$$\sigma = \frac{ne^2}{m^*(\omega^2+1/\tau^2)^{1/2}}\,\frac{\sin\psi}{(1+\gamma^2)^{1/2}}\,F\left(\tfrac{1}{2},\tfrac{1}{2};2;\frac{\gamma}{1+\gamma}\right) \tag{3.28}$$

and

$$\epsilon_1 = \epsilon_L - \frac{4\pi ne^2}{m^*\omega(\omega^2+1/\tau^2)^{1/2}}\,\frac{\cos\psi}{(1+\gamma^2)^{1/2}}\,F\left(\tfrac{1}{2},\tfrac{1}{2};2;\frac{\gamma}{1+\gamma}\right) \tag{3.29}$$

It should be noted that the electric field $\vec{E}$ appearing in Eq. (3.25) refers to the electric field within the semiconductor. We relate it to the incident field $\vec{E}_i$ in the usual way,

$$\vec{E} = \frac{2\vec{E}_i}{1+\epsilon^{1/2}} \tag{3.30a}$$

and obtain

$$\gamma = \gamma_i\left|\frac{2}{1+[\epsilon(\gamma,\omega)]^{1/2}}\right|^2\frac{1}{1+1/\omega^2\tau^2} \tag{3.30b}$$

where

$$\gamma_i = \left(\frac{e E_i}{m^* c^* \omega} \right)^2 \qquad (3.31)$$

Eqs. (3.19) and (3.28)-(3.31) are solved in a self consistent way to find ϵ . Then R is determined by Eq. (3.17).

Results for InSb :

The theory obtained above is now applied to a particular crystal of interest - InSb , which is chosen because its parameters result in large[47] nonlinear effects. The relevant parameters are $m^* = \frac{1}{60} m_e$ (m_e being the free electron's rest mass), $c^* = \frac{1}{270} c$ (c being the speed of light in vacuum), and $\epsilon_L = 16$. Results for reflectivity are obtained for various values of light intensity. Plasma frequency is taken to lie in the infrared region of the spectrum at $\omega_p = 0.1892 \times 10^{14}$ rad/sec. This corresponds to a carrier concentration of $n = 3 \times 10^{16}$ cm^{-3} . The phenomenological life time obtained from mobility measurements[41] is $\tau = 0.759 \times 10^{-12}$ sec.

In Fig. 7, the reflection efficiency R is plotted as a function of frequency for several values of light intensity. In all cases the curves display the precipitous drop at plasma frequency followed by a slow rise at high frequencies to some constant value determined by the mismatch of dielectric constants of the crystal and vacuum. For low intensities, the curves are as conventionally expected with the break at frequencies around ω_p , but for higher intensities there is a substantial shift of the break in the reflectivity towards lower frequencies. This is

consistent with the hypothesis that there is a local depression of the effective plasma frequency by the strong modulation of the electronic velocities at high light intensities.

One may think of the effect as an intensity induced transparency of the plasma. Naturally absorption will limit the extent of the transparency but the effect should be observable in thin film crystals. The transmission efficiency of the film should increase dramatically at frequencies below the plasma frequency if the intensity is increased sufficiently.

For comparison's sake, we calculate the reflectivities for the case where collisions are neglected and in Fig. 8 , plot the curves for the same intensities as in Fig. 7. The only effect is to sharpen up the step discontinuity at the plasma cut-off.

While we considered the case of linearly polarized light, it is clear that a parallel developement exists for circularly polarized light. The results are similar to those presented in Figs. 7 and 8. Thus nonlinear reflection is an important effect in narrow-band-gap semiconductors.

D. Nonlinear Pulse Propagation

Since nonlinearity has such a profound effect on the reflective properties of crystals, it is only expected that nonlinear transmission at high intensities of the radiation field should also exhibit anomalous behaviours. The phenomenon of self-induced transparency has been studied both for absorptive and dispersive media. In the latter case , attention has been limited to an analysis of the soliton pulse solution of the problem. Here we extend the study of pulse propagation to some simple boundary value problems. Our attention will again be limited to the narrow band-gap semiconductors.

It is slightly more convenient to analyse the circularly polarized case than the linearly polarized case here. Then as shown in Section B, the problem reduces to solving the following nonlinear equation for the vector potential $\vec{A}$:

$$\nabla^2 \vec{A} - \frac{\epsilon_L}{c^2} \frac{\partial^2 \vec{A}}{\partial t^2} = \frac{\epsilon_L \omega_p^2}{c^2} \vec{A} \left[1 + \left(\frac{eA}{m^* c^* c} \right)^2 \right]^{-1/2} \tag{3.32}$$

where

$$\frac{e\vec{A}}{m^* c^* c} = \alpha \left[\hat{i} \cos(kz - \omega t - \chi) + \hat{j} \sin(kz - \omega t - \chi) \right] \tag{3.33}$$

Here α and χ represent the amplitude and phase of the pulse. Owing to the nonlinear term on the right hand side of Eq. (3.32), it appears

difficult to obtain a general solution to the boundary value problem. Hence numerical integration was resorted to and the solutions were obtained for various boundary conditions.

In Fig. 9 we present results for the case of a pulse striking a crystal of a doped semiconductor . If the pulse impinges on the crystal from vacuum, then due to the hefty dielectric mismatch, a large part of the energy of the pulse will be reflected. To avoid this complication we imagine the pulse originally travelling in the pure semiconductor and then striking the doped portion. The carrier frequency of the pulse is taken to lie below the ambient plasma frequency of the medium. In this case, the ratio ω/ω_p was taken to be 0.5 and absorptive effects of the medium were neglected. The intensity of the pulse was chosen to correspond to the amplitude $(eA/m^*c^*c)_{max} = 20.0$.

One notes that the pulse enters the medium and quickly assumes the soliton behaviour. Since the medium is nonabsorptive, the semiconductor acts as a perfect transmitter of the soliton. Thus we have a rather drastic example of the self-induced transparency phenomenon. A small part of the pulse is reflected to the left, due, in part, to the residual mismatch of indices of refraction.

For comparison's sake and as a check on the numerical integration we present in Fig. 10 resultsfor the case when the nonlinearity on the right hand side of Eq. (3.32) is supressed (i.e. let $c^* \to \infty$). The other

parameters of the problem are same as in the previous case. Here one notices the conventional reflection without transmission since the frequency of the wave is below the plasma frequency. Penetration of the linear plasma occurs only upto a skin depth and self-induced transparency is not observed. The dispersion of the medium has completely blocked the passage of the pulse.

In Fig. 11 we examine the penetration of a pulse through a slab of doped semiconductor for the same values of the parameters as in Fig. 9. The thickness of the slab was taken to be 60λm. One notices almost 100% transmission efficiency, the small reflection again being due to residual mismatch of refractive indices. This behaviour is to be contrasted with Fig. 12 where the same computation was made for a lower amplitude. Here there is practically total reflection. It was found that for values of $(eA/m^{*}c^{*}c)_{max}$ less than 7.0 , no self induced transparency occured. This can be understood by the following line of reasoning. We have seen that the local plasma frequency is depressed by an intense pulse. Propagation can occur only if the depressed plasma frequency lies below the carrier frequency of the pulse. Thus, we have a critical value of the peak intensity for self-induced transparency to occur, determined by the mismatch of ω and ω_p . This value can be found by the use of the dispersion formula obtained in Eq.(3.15) as,

$$\omega^2 = \frac{k^2c^2}{\epsilon_L} + \frac{2\omega_p^2}{1+\left(1+\frac{1}{16}U^2\right)^{1/2}}$$

where

$$U = \int_{-\infty}^{+\infty} \alpha^2 \, d\xi$$

For $\omega/\omega_p = 0.5$, the critical value for $(eA/m^*c^*c)_{max}$ is 7.0 and Fig. 12 was plotted for a lesser value, namely $(eA/m^*c^*c)_{max} = 6.0$.

In actual practice, the absorptivity of the medium does not allow us to draw such sharp conclusions. One must then think in terms of anomalously large penetration depths rather than total self-induced transparency. The transmission properties of a slab will still exhibit a marked discontinuity but the maximum efficiency will be limited to $e^{-\gamma L}$, where γ is the absorption coefficient and L is the thickness of the slab.

As an illustration of the case where absorption is present, we present in Fig. 13, the pulse propagating in an absorptive medium. The absorption was tacked on to the theory in a phenomenological way by introducing a conductivity to the medium. The wave equation thus becomes

$$\nabla^2\vec{A} - \frac{\epsilon_L}{c^2}\frac{\partial^2\vec{A}}{\partial t^2} - \frac{\epsilon_L}{c^2\tau}\frac{\partial\vec{A}}{\partial t} = \frac{\epsilon_L\omega_p^2}{c^2}\vec{A}\left[1+\left(\frac{eA}{m^*c^*c}\right)^2\right]^{-1/2} \tag{3.34}$$

In this equation τ represents an empirical collision life time. Here we took $\omega_p\tau = 20.0$, which is a realistic estimate for InSb[48].

One observes that the pulse is able to propagate without dispersion

but that it attenuates with time, much as expected. There is a tendency for the pulse to compress itself in time as the propagation occurs. This is due to the fact that it tries to keep its peak intensity above the critical value for self-induced transparency to occur, as long as possible.

CHAPTER IV

Four Photon Parametric Amplification in Semiconductors

A. Introduction

Much interest has been shown in recent years in devising new techniques for obtaining coherent tunable electromagnetic energy. In particular, Patel and Shaw[17] have introduced the Raman spin-flip laser which is capable of generating tunability over a wide range of the infrared spectrum. The experiment involves the Raman scattering of a primary laser beam in a sample of narrow band gap semiconductor embedded in a magnetic field[49-52].

Here we explore an alternate method for generating infrared radiation by employing a four photon parametric process using the same type of semiconductor. We expect this process to generate infrared radiation in a more extended frequency range than currently available.

Interest in parametric phenomena and four photon processes stems from the work of Giordimaine[53] and De Martini and Kelley[54]. The basic technique that is proposed here is to allow two primary laser beams to interact in the narrow gap semiconductor in the presence of a magnetic field. The nonlinear response of the medium, originating from the non-parabolic dispersion of the conduction electrons generates the current density which acts as a parametric pump for the two secondary beams. By appropriately tuning the cavity, it is possible to frequency select particular modes that have undergone parametric growth. The purpose of the magnetic

field is to allow phase matching to be achieved in a collinear geometry, as well as to produce a cyclotron resonant enhancement of the amplification. It is found that the parametric growth can be quite substantial and a practical and efficient means for obtaining tunable infrared radiation may be obtained by employing this technique.

In section B, we outline the basic theoretical considerations relating to the parametric process and derive a formula for the growth rate of the secondary waves. In section C, the phase matching criteria are studied and the limitations they set on the frequencies are obtained. Finally, section D deals with the numerical results and a discussion of the process.

B. Parametric Amplification

Consider the case of a narrow band gap semiconductor embedded in a dc magnetic field $\vec{B}$ directed along the $-z$ axis. If the sample is irradiated with circularly polarized light along $\hat{z}$, the equation of motion of an electron with electronic charge $-e$ and effective mass m^* at the bottom of the conduction band can be written as[27]

$$\left(\frac{d}{dt} + \frac{1}{\tau} \right) \frac{m^* \vec{v}}{\left[1 - (v/c^*)^2 \right]^{1/2}} = -e \left[\vec{E} + \frac{\vec{v}}{c} \times \vec{B} \right] \qquad (4.1)$$

where $\vec{v}$ is the electronic velocity, $c^* = (E_g / 2m^*)^{1/2}$ where E_g is the gap energy, and τ is a phenomenological relaxation time. $\vec{E}$ is the ac electric field of the incident radiation and in calculating the electron dynamics, we have neglected the Lorentz force of the ac magnetic field and the $(\vec{v}.\nabla)\vec{v}$ term since typical electronic speeds are much less than the speed of light.

In terms of the vector potential $\vec{A}$, which is a circularly polarized vector and a dimensionless velocity $\vec{u} = \vec{v}/c$, also a circularly polarized vector, the equation becomes,

$$\left(\frac{d}{dt} + \frac{1}{\tau} \right) \frac{\vec{u}}{(1-u^2)^{1/2}} = \mu \frac{d\vec{A}}{dt} + i\omega_c \vec{u} \qquad (4.2)$$

where $\mu = e/m^* c^* c$ and the cyclotron frequency $\omega_c = eB/m^* c$.

While considering the parametric conversion of frequencies ω_1 and ω_2 into ω_3 and ω_4, the total vector potential $\vec{A}$ is taken to consist of the sum of the vector potentials due to the four frequencies :

$$\vec{A} = \sum_{\nu=1}^{4} \hat{e} A_\nu \exp\left[-i (k_\nu z - \omega_\nu t - \chi_\nu) \right] \qquad (4.3)$$

where χ_ν are the phase factors, k_ν are the propagation vectors and $\hat{e} = (\hat{x} + i\hat{y})$ is the circularly polarized vector so that

$$\hat{e}.\hat{e} = \hat{e}^*.\hat{e}^* = 0$$

and

$$\hat{e}^*.\hat{e} = \hat{e}.\hat{e}^* = 2. \tag{4.4}$$

The propagation vectors k_ν are taken to be complex to allow for growth, depletion or absorption due to collisions. Since we are interested in the parametric growth of ω_3 and ω_4, we separate the real and the imaginary parts of k_3 and k_4 and write

$$k_3 = q + i\gamma \tag{4.5a}$$

and

$$k_4 = p + i\gamma \tag{4.5b}$$

We solve the equation of motion given by Eq. (4.2) in terms of the power series :

$$\vec{u} = \mu \vec{U}_1 + \mu^3 \vec{U}_2 + \ldots \tag{4.6}$$

On substituting Eq. (4.6) into Eq. (4.2), the equation of motion, to the first order, becomes,

$$\frac{d\vec{U}_1}{dt} + \frac{\vec{U}_1}{\tau} = \frac{d\vec{A}}{dt} + i\omega_c \vec{U}_1 \tag{4.7}$$

and the first order solution is easily obtained as,

$$\vec{U}_1 = \sum_{\nu=1}^{4} \hat{e}\, U_{1\nu} \exp\left[-i(k_\nu z - \omega_\nu t - \chi_\nu)\right] \tag{4.8a}$$

where

$$U_{1\nu} = \frac{\omega_\nu A_\nu}{\Delta_\nu^2}\left(\omega_\nu - \omega_c + \frac{i}{\tau}\right) \tag{4.8b}$$

and

$$\Delta_\nu^2 = (\omega_\nu - \omega_c)^2 + \frac{1}{\tau^2} \tag{4.8c}$$

The second order solution is obtained by solving

$$\left(\frac{d}{dt} + \frac{1}{\tau}\right)\left[\vec{U}_2 + \tfrac{1}{2}\vec{U}_1(\vec{U}_1 \cdot \vec{U}_1)\right] = i\omega_c \vec{U}_2 \tag{4.9}$$

The presence of the $\frac{1}{2}\vec{U}_1(\vec{U}_1 \cdot \vec{U}_1)$ term shows that $\vec{U}_2$ will contain many mixed frequency components, each of which will act as a source term for the growth of that particular frequency. However, we are only interested in the parametric growth of ω_3 and ω_4 components . Therefore, instead of blindly solving Eq.(4.9) for all components, we only look for ω_3 and ω_4 parts of $\vec{U}_2$. These components are written respectively as,

$$U_{23}\,\hat{e}\,\exp.\left[-i(K_3 z - \omega_3 t - \chi_3)\right] \quad \text{and} \quad U_{24}\,\hat{e}\,\exp.\left[-i(K_4 z - \omega_4 t - \chi_4)\right]$$

where U_{23} and U_{24} may be complex to allow for the phase difference.

Then, the equation for the ω_3 component of $\vec{U}_2$ is obtained as

$$\left(\frac{d}{dt} + \frac{1}{\tau}\right)\left\{U_{23} + \tfrac{1}{2}|U_{13}|^2 U_{13} + U_{11}U_{12}U_{14}^*\exp.\left[i(\chi_1 + \chi_2 - \chi_3 - \chi_4)\right]\right\}$$

$$\times \exp\left[-i(K_3 z - \omega_3 t - \chi_3)\right] = i\omega_c U_{23}\exp.\left[-i(K_3 z - \omega_3 t - \chi_3)\right] \tag{4.10}$$

where we have used the fact that the four photon parametric process , in going from ω_1 and ω_2 into ω_3 and ω_4 obeys the energy and momentum conservation relations given, respectively, by

$$\omega_1 + \omega_2 = \omega_3 + \omega_4 \tag{4.11a}$$

$$K_1 + K_2 = K_3^* + K_4 = K_3 + K_4^* = q_\parallel + p \tag{4.11b}$$

Eq.(4.10) is easily solved to obtain,

$$U_{23} = -\frac{(\omega_3 - \frac{i}{\tau})(\omega_3 - \omega_c + \frac{i}{\tau})}{\Delta_3^2}\left\{\frac{1}{2}|U_{13}|^2 U_{13} + U_{11}U_{12}U_{14}^* \exp[i(\chi_1 + \chi_2 - \chi_3 - \chi_4)]\right\}$$

The phase factors χ_ν are the initial phase factors and are determined by the experimental setup. If the initial conditions are chosen such that

$$\chi_1 + \chi_2 = \chi_3 + \chi_4 + \frac{\pi}{2}\,, \tag{4.12}$$

the expression for U_{23} becomes,

$$U_{23} = -\frac{(\omega_3 - \frac{i}{\tau})(\omega_3 - \omega_c + \frac{i}{\tau})}{\Delta_3^2}\left(\frac{1}{2}|U_{13}|^2 U_{13} + i\,U_{11}U_{12}U_{14}^*\right).$$

The ω_3 component of the electron velocity is therefore given by,

$$\hat{e}\,\mu c^*\left[U_{13} + \mu^2 U_{23}\right]\exp\left[-i(K_3 z - \omega_3 t - \chi_3)\right]$$

$$= \hat{e}\,\mu c^*\left\{\frac{\omega_3 A_3}{\Delta_3^2}(\omega_3 - \omega_c + \frac{i}{\tau}) - \mu^2\,\frac{(\omega_3 - \frac{i}{\tau})(\omega_3 - \omega_c + \frac{i}{\tau})}{\Delta_3^2}\right.$$

$$\times\left[\frac{1}{2}\frac{\omega_3^3 A_3^3}{\Delta_3^4}(\omega_3 - \omega_c + \frac{i}{\tau}) + \frac{i\,\omega_1\omega_2\omega_4 A_1 A_2 A_4}{\Delta_1^2\Delta_2^2\Delta_4^2}(\omega_1 - \omega_c + \frac{i}{\tau})(\omega_2 - \omega_c + \frac{i}{\tau})\right.$$

$$\left.\left.\times(\omega_4 - \omega_c - \frac{i}{\tau})\right]\right\}\exp\left[-i(K_3 z - \omega_2 t - \chi_3)\right]$$

where we have substituted for $U_{1\nu}$'s from Eq.(4.8). Using this velocity as the source of ω_3 frequency current in the wave equation,

$$\frac{\partial^2 \vec{A}}{\partial z^2} - \frac{\epsilon_L}{c^2}\frac{\partial^2 \vec{A}}{\partial t^2} = -\frac{4\pi}{c}\vec{J}\,, \tag{4.13}$$

where ϵ_L is the lattice dielectric function, we obtain the equation for the ω_3 frequency as,

$$\left(-K_3^2+\frac{\epsilon_L}{c^2}\omega_3^2\right)A_3=\Bigg[\frac{\omega_3 A_3}{\Delta_3^2}\left(\omega_3-\omega_c+\frac{i}{\tau}\right)-\frac{\mu^2}{2}\frac{\left(\omega_3-\frac{i}{\tau}\right)\left(\omega_3-\omega_c+\frac{i}{\tau}\right)^2(\omega_3 A_3)^3}{\Delta_3^6}$$

$$-i\mu^2\frac{\omega_1\omega_2\omega_4}{\Delta_1^2\Delta_2^2\Delta_3^2\Delta_4^2}\left(\omega_1-\omega_c+\frac{i}{\tau}\right)\left(\omega_2-\omega_c+\frac{i}{\tau}\right)$$

$$\times\left(\omega_3-\omega_c+\frac{i}{\tau}\right)\left(\omega_4-\omega_c+\frac{i}{\tau}\right)\left(\omega_3-\frac{i}{\tau}\right)A_1A_2A_4\Bigg]\frac{\omega_p^2\epsilon_L}{c^2}$$

(4.14)

where $\omega_p^2 = 4\pi ne^2/m^*\epsilon_L$ is the plasma frequency, with n the concentration of electrons in the conduction band.

Eq.(4.14) describes the parametric growth of frequency ω_3 . As expected for a four-photon parametric process, the equation has a term proportional to A_4 . Similarly, the equation for A_4 would contain a term proportional to A_3. Using Eq.(4.5a) in Eq. (4.14), equating the real parts on both sides, and keeping only the lowest order terms in $1/\tau$, one gets

$$q^2A_3=\frac{\epsilon_L}{c^2}\Bigg(\omega_3^2-\frac{\omega_p^2\omega_3(\omega_3-\omega_c)}{\Delta_3^2}$$

$$+\mu^2\frac{\omega_p^2}{2}\frac{\left[\omega_3\left\{(\omega_3-\omega_c)^2-\frac{1}{\tau^2}\right\}+\left(\frac{2}{\tau^2}\right)(\omega_3-\omega_c)\right]\omega_3^3A_3^2}{\Delta_3^6}\Bigg)A_3$$

$$+\frac{\omega_p^2\epsilon_L}{c^2\tau}\mu^2\omega_1\omega_2\omega_4A_1A_2A_4\left[\omega_3\left(\frac{1}{\omega_1-\omega_c}+\frac{1}{\omega_2-\omega_c}+\frac{1}{\omega_3-\omega_c}+\frac{1}{\omega_4-\omega_c}\right)-1\right]$$

$$\times(\omega_1-\omega_c)(\omega_2-\omega_c)(\omega_3-\omega_c)(\omega_4-\omega_c)\left(\Delta_1\Delta_2\Delta_3\Delta_4\right)^{-2} \qquad (4.15)$$

where γ^2 has been neglected compared to q^2. Eq. (4.15) is essentially the dispersion relation for ω_3 with small corrections due to absorption, nonlinearity and parametric effects. In fact, in the limit $\tau \to \infty$, Eq.(4.15) reduces to,

$$q^2 = \frac{\epsilon_L \omega_3^2}{c^2}\left(1 - \frac{\omega_p^2}{\omega_3^2}\frac{1}{(1-\omega_c/\omega_3)} + \frac{1}{2}\mu^2 A_3^2 \frac{\omega_p^2}{\omega_3^2}\frac{1}{(1-\omega_c/\omega_3)^4}\right),$$

which is really the nonlinear dispersion relation obtained before as Eq. (2.19) in our discussion on self focusing in semiconductors.

Similarly, equating the imaginary terms on both sides of Eq.(4.14) and keeping only the lowest order terms in $1/\tau$, one obtains,

$$-2q\gamma_3 A_3 = \frac{\omega_p^2 \epsilon_L}{c^2}\left(\frac{\omega_3 A_3}{\tau \Delta_3^2} - \frac{\mu^2}{2\tau}\frac{(\omega_3^2-\omega_c^2)}{\Delta_3^6}(\omega_3 A_3)^3 - \frac{\mu^2 \omega_1\omega_2\omega_3\omega_4}{(\Delta_1\Delta_2\Delta_3\Delta_4)^2}(\omega_1-\omega_c)(\omega_2-\omega_c)(\omega_3-\omega_c)(\omega_4-\omega_c)A_1A_2A_4\right).$$

The A_3^3 term can be dropped compared to the $A_1A_2A_4$ term since A_1 and A_2 are large, being pumped, while A_3 and A_4 , the parametrically produced outputs will be relatively small. Also , the first term on the right hand side is interpreted as arising due to the linear absorption of the frequency ω_3 . Introducing the linear absorption coefficient $\alpha_3 = \omega_p^2 \epsilon_L \omega_3 / 2c^2 \Delta_3^2 \tau q$, the equation for γ becomes,

$$(\gamma+\alpha_3)A_3 = \frac{\omega_p^2 \epsilon_L \mu^2}{2qc^2}\frac{\omega_1\omega_2\omega_3\omega_4}{(\Delta_1\Delta_2\Delta_3\Delta_4)^2}(\omega_1-\omega_c)(\omega_2-\omega_c)(\omega_3-\omega_c)(\omega_4-\omega_c)A_1A_2A_4.$$

(4.16a)

Proceeding in an analogous way for the ω_4 frequency, one obtains,

$$(\gamma+\alpha_4)A_4 = \frac{\omega_p^2 \epsilon_L \mu^2}{2qc^2}\frac{\omega_1\omega_2\omega_3\omega_4}{(\Delta_1\Delta_2\Delta_3\Delta_4)^2}(\omega_1-\omega_c)(\omega_2-\omega_c)(\omega_3-\omega_c)(\omega_4-\omega_c)A_1A_2A_3$$

(4.16b)

where α_4 is the linear absorption coefficient for ω_4.

Combining Eqs. (4.16a) and (4.16b) to eliminate A_3A_4 results in

$$\gamma = -\tfrac{1}{2}(\alpha_3+\alpha_4) + \tfrac{1}{2}\left[(\alpha_3-\alpha_4)^2 + \frac{4}{pq}\left(\frac{\omega_p^2\epsilon_L}{2c^2}\frac{\omega_1\omega_2\omega_3\omega_4}{(\Delta_1\Delta_2\Delta_3\Delta_4)^2}\right.\right.$$
$$\left.\left.\times(\omega_1-\omega_c)(\omega_2-\omega_c)(\omega_3-\omega_c)(\omega_4-\omega_c)A_1A_2\right)^2\right]^{1/2}, \tag{4.17}$$

which gives the parametric growth rate.

For $\tau \to \infty$, i.e., no absorption, the growth rate will always be positive But for finite τ, one needs a threshold value for the product $\vec{A}_1\vec{A}_2$ only above which the parametric growth will take place. Also, the growth depends on the product A_1A_2 and not individually on the vector potentials A_1 and A_2 for the two primary beams. It should be noted that the product A_1A_2 appearing in Eq. (4.17) refers to the vector potentials inside the semiconductor and is different from the potential outside. We relate it to the incident field in the usual way (see Eq. (3.30)) and in terms of the mean incident intensity I_i, we can write,

$$A_1A_2 = \frac{8\pi c}{\omega_1\omega_2} I_i \frac{2}{1+[\epsilon(\omega_1)]^{1/2}} \cdot \frac{2}{1+[\epsilon(\omega_2)]^{1/2}} \tag{4.18}$$

where $I_i = (I_{1i}I_{2i})^{1/2}$, I_{1i} and I_{2i} being the incident intensities for ω_1 and ω_2 beams respectively.

Letting $\gamma \to 0$ in Eq. (4.17) and using Eq. (4.18), the threshold value of the mean incident intensity is given by :

$$(I_i)_{th} = \frac{1+[\epsilon(\omega_1)]^{1/2}}{2} \frac{1+[\epsilon(\omega_2)]^{1/2}}{2} \frac{\Delta_1^2 \Delta_2^2 \Delta_3 \Delta_4}{8\pi c \mu^2 (\omega_3\omega_4)^{1/2} \tau}$$

$$\times \left[(\omega_1-\omega_c)(\omega_2-\omega_c)(\omega_3-\omega_c)(\omega_4-\omega_c) \right]^{-1}$$

(4.19)

Only when the mean incident intensity exceeds the above value will the parametric amplification of ω_3 and ω_4 waves take place. Exactly at threshold, the growth will just be balanced by the linear attenuation.

C. Phase Matching

In the process of parametric amplification through four photon interaction, the two incident photons combine in such a way as to parametrically pump two other photons. Phase matching is the requirement that energy and momentum conservation conditions are simultaneously satisfied. In general, the pumped photons will not always travel along the direction of the incident beams, resulting in a non-colinear process requiring complicated theoretical and experimental analysis. However by the appropriate use of a dc magnetic field, it is possible to alter the dielectric properties of the semiconductor in such a way as to achieve phase matching along the beam. This leads to a coherent loss mechanism in which the pumped waves grow along the length of the primary beams as was considered in the previous section. It was for this reason that the momentum conservation condition, Eq. (4.11b), was a scalar equation, since all the four waves propagate along the $\hat{z}$ direction. We now proceed to obtain the requirements on the magnetic field for colinear phase matching to be possible.

Since phase matching is essentially a correction to the parametric process, it suffices to take the dispersion relation without absorption and nonlinearity and write it in the usual form in the presence of a magnetic field :

$$K^2 = \epsilon_L \frac{\omega^2}{c^2} \left(1 - \frac{\omega_p^2/\omega^2}{1 - \omega_c/\omega} \right) . \qquad (4.20)$$

Using Eq. (4.20) , we can approximate the dispersion relations for the four frequencies by the equations,

$$
\begin{aligned}
K_1 &= \frac{\omega_1 \epsilon_L^{1/2}}{c}\left(1-\frac{\omega_p^2/\omega_1^2}{2(1-\omega_c/\omega_1)}\right)\\
K_2 &= \frac{\omega_2 \epsilon_L^{1/2}}{c}\left(1-\frac{\omega_p^2/\omega_2^2}{2(1-\omega_c/\omega_2)}\right)\\
q &= \frac{\omega_3 \epsilon_L^{1/2}}{c}\left(1-\frac{\omega_p^2/\omega_3^2}{2(1-\omega_c/\omega_3)}\right)\\
p &= \frac{(\omega_1+\omega_2-\omega_3)\epsilon_L^{1/2}}{c}\left(1-\frac{\omega_p^2/(\omega_1+\omega_2-\omega_3)^2}{2\left[1-\omega_c/(\omega_1+\omega_2-\omega_3)\right]}\right)
\end{aligned}
\tag{4.21}
$$

where, we have made use of the energy conservation relation given by Eq. (4.11a) to eliminate ω_4.

Using Eqs. (4.21) in the momentum conservation condition , Eq. (4.11b), results in the simple phase matching condition,

$$\omega_c = \tfrac{1}{2}(\omega_1 + \omega_2) \quad . \tag{4.22}$$

Another requirement for succesful parametric amplification is that all the waves be able to propagate through the semiconductor. In other words , the dielectric function $\epsilon(\omega_\nu)$, given by

$$\epsilon(\omega_\nu) = \epsilon_L\left[1-\frac{\omega_p^2/\omega_\nu^2}{1-\omega_c/\omega_\nu}\right] \tag{4.23}$$

should be positive for all ω_ν. When $\epsilon(\omega_\nu)$ is plotted as a function of ω_ν , one finds that for $\omega_p^2/\omega_\nu^2 \ll 1$, $\epsilon(\omega_\nu)$ is negative only

in the range $\omega_c < \omega_\nu < \omega_c + \omega_p^2/\omega_c$.

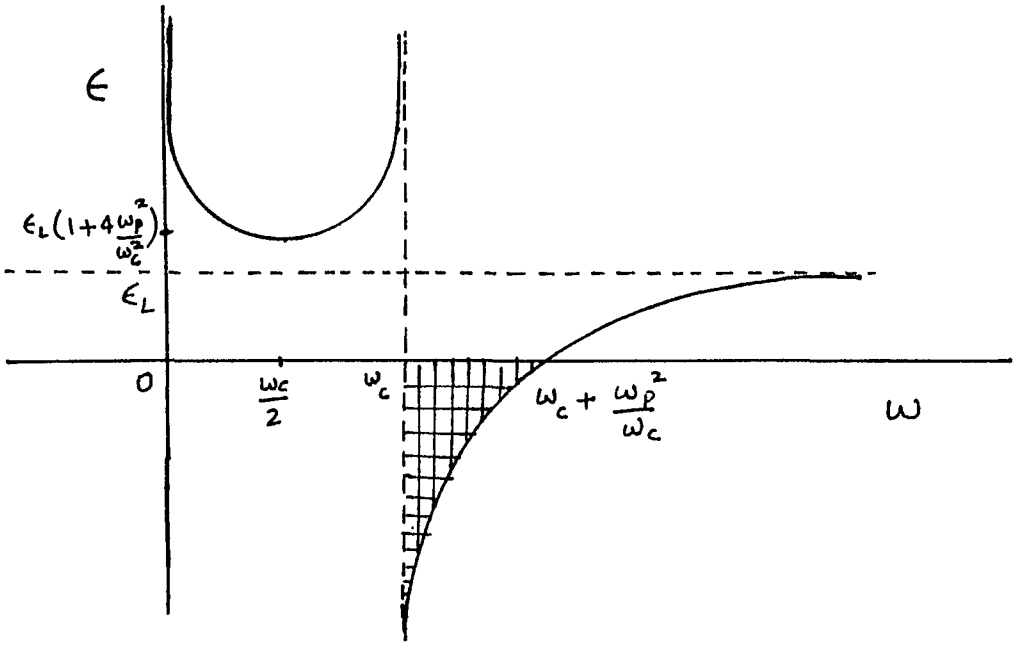

Therefore if we choose the frequencies such that $\omega_1 < \omega_c < \omega_2$ and $\omega_3 < \omega_4$, the use of the phase matching requirement given by Eq.(4.22) results in the following requirement for $\epsilon(\omega_\nu)$ to be positive :

$$4\omega_p^2 < \omega_2^2 - \omega_1^2 \tag{4.24a}$$

and

$$\omega_3 < \omega_c - \omega_p^2/\omega_c \tag{4.24b}$$

It is to be noted that the requirement for $\epsilon(\omega_4)$ to be positive is included in the above. ω_4 does not appear explicitly in the above inequalities since choosing ω_3 immediately fixes ω_4, as required by Eq. (4.11a). Eqs. (4.22)and (4.24) together with Eq. (4.11a) represent all the restrictions on the freqùencies for complete phase match and

possibility of propagation through the semiconductor.

Using Eqs. (4.22) and (4.11a), the expression given by Eq. (4.17) for the growth parameter γ can be rewritten in the limit $\tau \to \infty$,

$$\gamma = \frac{1}{2}\frac{\omega_p^2 \epsilon_L^{1/2}}{c}\left(\frac{e}{m^* c^* c}\right)^2 \frac{A_1 A_2 \omega_1 (2\omega_c - \omega_1)\omega_3^{1/2}(2\omega_c - \omega_3)^{1/2}}{(\omega_1 - \omega_c)^2(\omega_3 - \omega_c)^2}$$

$$\times\left[\left(1 - \frac{\omega_p^2/\omega_3^2}{2(1-\omega_c/\omega_3)}\right)\left(1 - \frac{\omega_p^2/(2\omega_c - \omega_3)^2}{2[1-\omega_c/(2\omega_c-\omega_3)]}\right)\right]^{-\frac{1}{2}} \quad (4.25)$$

where, we have substituted for p and q from Eq. (4.21). Eq. (4.25) gives the growth rate for parametric amplification in the absence of absorptions due to collisions.

D. Results and Discussion

In the previous sections, a theory was derived for four photon parametric amplification in semiconductors. The nonlinearity associated with the nonparabolicity of the conduction band was responsible for the four photon process. Two incident lasers at frequencies ω_1 and ω_2 were allowed to interact to parametrically drive two output beams at frequencies ω_3 and ω_4. A magnetic field was utilized for two reasons. First it permitted one to obtain phase matching in a linear geometry, i.e. all the four beams could be colinear. In addition, it lead to a cyclotron enhancement of the nonlinear effect itself. The latter effect has already been employed in Chapter II and other discussions [55] relating to nonlinear propagation in narrow gap semiconductors.

In Fig. 14, the growth rate given by Eq.(4.17) is plotted as a function of one of the parametrically pumped waves at frequency ω_3. The input frequencies ω_1 and ω_2 are denoted by arrows on the abcissa, as is their mean, which equals the cyclotron frequency ω_c. The values of the growth rate are given for two plasma frequencies ($\omega_p = 3.0 \times 10^{12}$ and 1.742×10^{12} rad / sec) and two mean incident laser intensities ($I_i = 10^7$ and 10^6 W/cm^2). The calculations were performed for InSb which was chosen for its low energy gap and low effective electron mass. Employing parameters for InSb ($E_g = 0.234$ eV , $m^* = m_e / 60$ and $\epsilon_L = 16$), the doping densities for curves A and C were $n = 7.56 \times 10^{14}$ cm^{-3} while for curves B and D, $n = 2.55 \times 10^{14}$ cm^{-3}.

The ω_c corresponds to a magnetic field of 152 KGauss.

One notes that the growth rate is quite substantial, particularly in the region near ω_c . One main limitation on the growth rate is the short photon mean free path, especially at frequencies close to ω_c because of resonant absorption. At these frequencies, the finite electron lifetime τ results in a larger linear absorption thus reducing significantly the optical absorption length or the photon mean free path. For this reason, the plasma frequencies were so chosen that the mean free path λ for frequencies ω_1 and ω_2 was of the order of a reasonable sample size (λ =1.24 cm for $\omega_p = 3.0 \times 10^{12}$ rad/sec and λ =4.83 cm for $\omega_p = 1.742 \times 10^{12}$ rad/sec) and ω_3 and ω_4 were not allowed to get any closer to ω_c than ω_1 and ω_2 . Thus for these sample sizes for all the four frequencies, the photon mean free path is at least the sample length.

In Fig. 15 , a similar plot of the growth rate is given for different values of ω_1 and ω_2 . The strong rise of the growth rate in the vicinity of ω_c can be understood simply in terms of the cyclotron resonance enhancement of the nonlinear coupling. Compared to the values in Fig. 14, ω_1 and ω_2 here are much closer to each other and hence to ω_c , resulting in much larger values of the growth rate than in Fig.14. The value of ω_c here corresponds to a magnetic field of 144 KGauss, other parameters being the same as in Fig 13. The lowest (out of the four frequencies) mean free paths were λ =

0.21 cm for $\omega_p = 3.0 \times 10^{12}$ rad / sec and $\lambda = 0.82$ cm for $\omega_p = 1.742 \times 10^{12}$ rad / sec.

In Figs. 16 and 17, the threshold value of the mean incident intensity $(I_i)_{th}$ given by Eq. (4.19) is plotted as a function of ω_3 for the frequencies and other parameters of Figs. 14 and 15 respectively. A high growth rate, especially near ω_c, results in relatively low values of $(I_i)_{th}$. As expected, thresholds values increase with increasing ω_p and are much lower for the parameters of Fig 17 where the growth rate is larger. At these intensities, the parametric growth will just be balanced by linear absorption. Much higher intensities are required for the parametrically pumped ω_3 and ω_4 beams to be experimentally observable.

In Figs. 14-17, the entire domain of values of ω_3 has been considered. But in practice, for InSb, the growth of the values beyond 10.6 μ will be restricted because of two photon absorption cutoff at high frequencies. Since the same absorption takes place for ω_4 also, there is also a cutoff at low frequencies because of Eq. (4.11 a). For these reasons, the parametric output is really limited to a frequency band whose width depends upon the parameters of the sample. The output frequency band can be expanded by the use of wider gap crystals. The particular output frequency required is obtained by appropriate tuning of the output cavity to select ω_3. Because of the high growth rates achieved here, the output lasers with extended frequency range

would be valuable spectroscopic tools. The input frequencies used here are currently available through various tunable laser devices like the spin-flip laser [17].

It should be noted that the choice of wavelengths around 10μ was taken as an example to illustrate the parametric process and the theory is not limited to these wavelengths. The parametric process described here can be used to extend the range of tunable lasers to other domains like the far infrared region. Here one must work in a pulse situation where typical intensities of $1\text{-}5 \times 10^6$ W/cm^2 can be achieved. For the far infrared region, the magnetic fields needed are much smaller than considered before, so there is no problem there. The three important parameters to consider are the incident intensity I_i, the laser frequency ω, and the electron density n. For an order of magnitude estimate, let us omit the magnetic field to simplify matters. Then the growth parameter is essentially given by $\gamma = \gamma_1 - \gamma_2$ where γ_1, the growth parameter in the absence of linear attenuation is proportional to $\frac{\omega}{c} \frac{\omega_p^2}{\omega^2} \left(\frac{eE}{m^* c^* \omega} \right)^2$ while γ_2, the linear attenuation, varies as $\frac{\omega}{c} \frac{\omega_p^2}{\omega^3 \tau}$. Thus for the purpose of scaling, we can write

$$\gamma = \frac{C n I_i}{\omega^3} - D \frac{n^2}{\omega^2} \qquad (4.26)$$

since ω_p^2 varies linearly with n. For illustrative purposes, we have taken $1/\tau$ to be proportional to n as for the case of Coulomb electron-ion scattering situation. (The estimate can be extended to cases where other scattering mechanisms are involved.)

Now take the case of 10μ versus a 100μ laser at the incident

frequencies. From Eq. (4.26) one simply ontains that on taking $n_{100} = \frac{1}{10} n_{10}$ and $I_{100} = \frac{1}{100} I_{10}$, the growth rates obey

$$\gamma_{10} = \gamma_{100} .$$

(Here the subscripts are self-explanatory.) Both the density n_{100} and the intensity I_{100} are within available range. Thus the high growth rate would make it possible to design tunable far infrared lasers.

In conclusion, in this chapter we have discussed a four photon parametric process with collinear phase matching and cyclotron resonance enhancement through a dc magnetic field and have shown that the resulting device would be a new type of laser source in a frequency domain like far infrared not currently available.

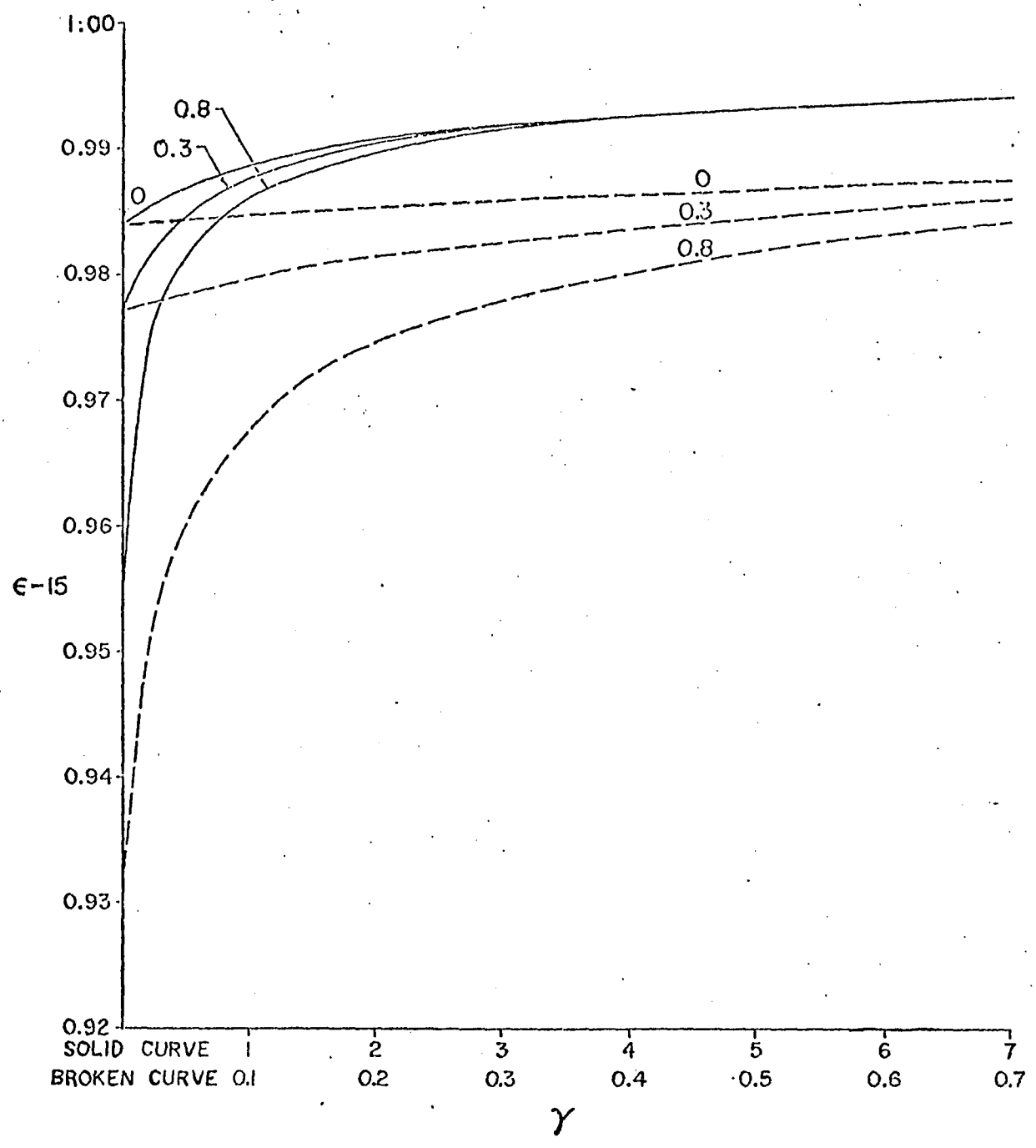

FIG. 1. Nonlinear dielectric function as a function of the power parameter γ for $\omega_c/\omega = 0, 0.3, 0.8$.

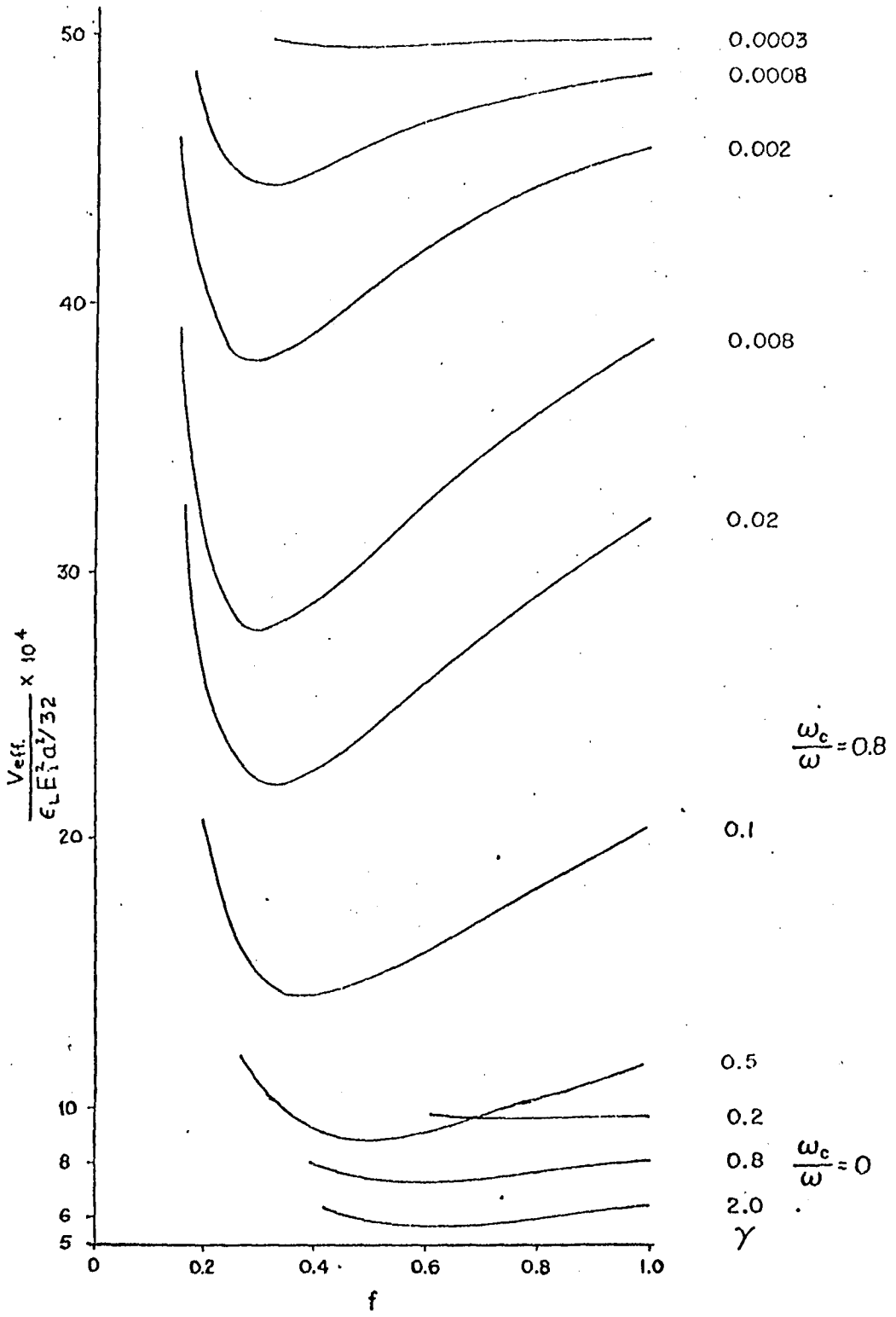

FIG. 2. Effective potential as a function of the dimensionless width f of the beam. Curves are drawn for various γ values for $\omega_c/\omega = 0, 0.8$.

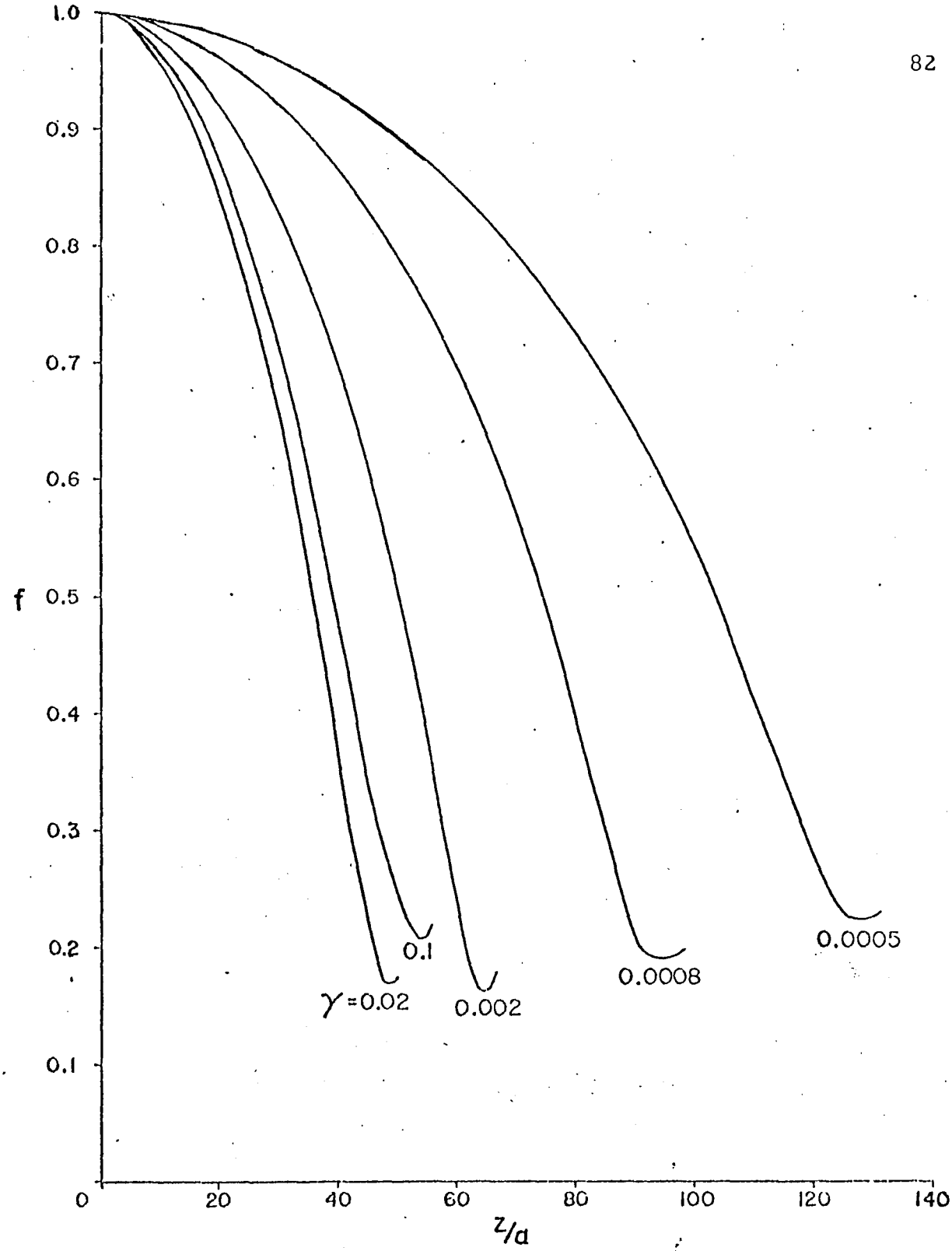

FIG. 3. Dimensionless beam radius f as a function of dimensionless distance z/a along the beam for $\omega_c/\omega = 0.8$ and for various γ values.

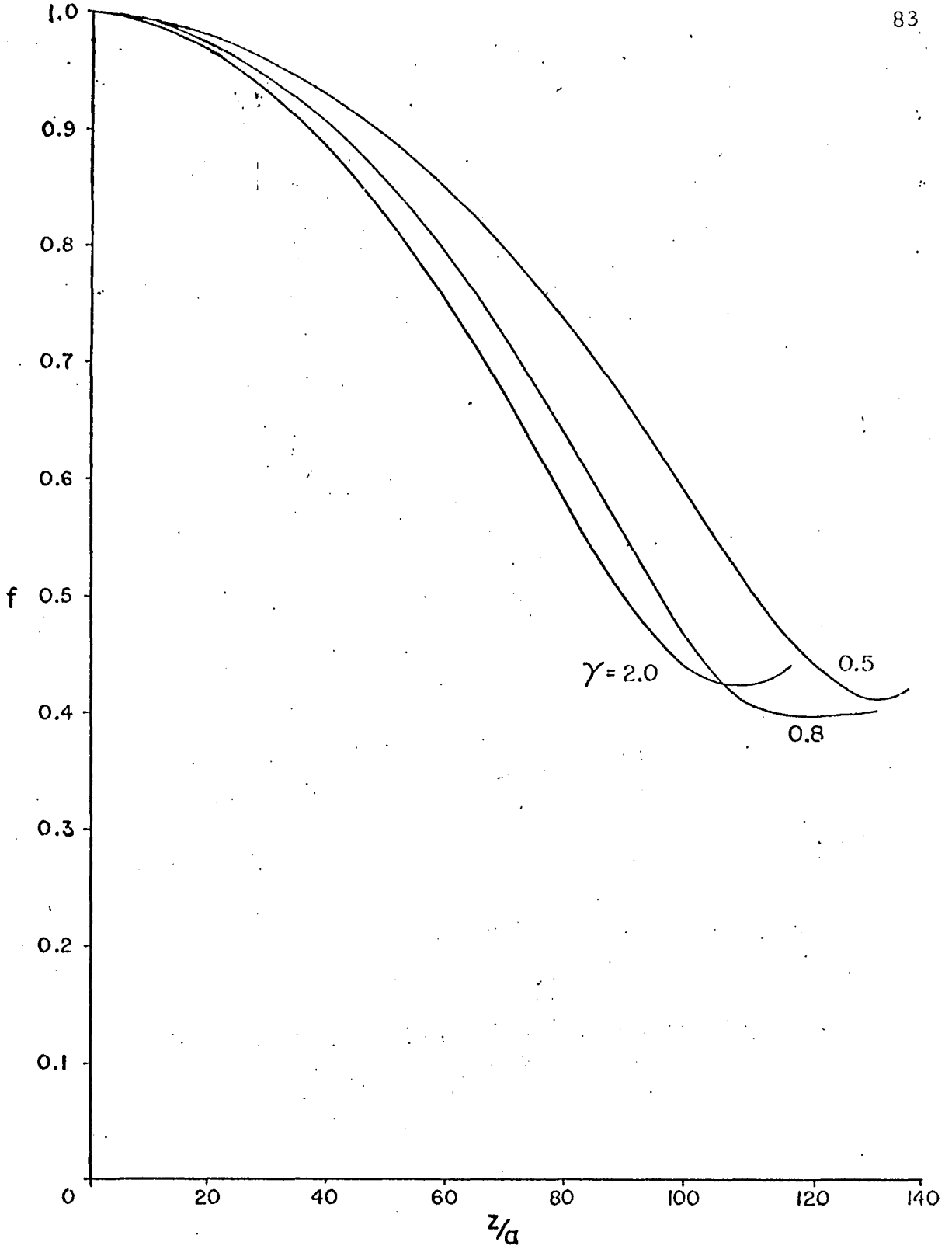

FIG. 4. Dimensionless beam radius f as a function of dimensionless distance z/a along the beam for $\omega_c/\omega = 0$ for various γ values.

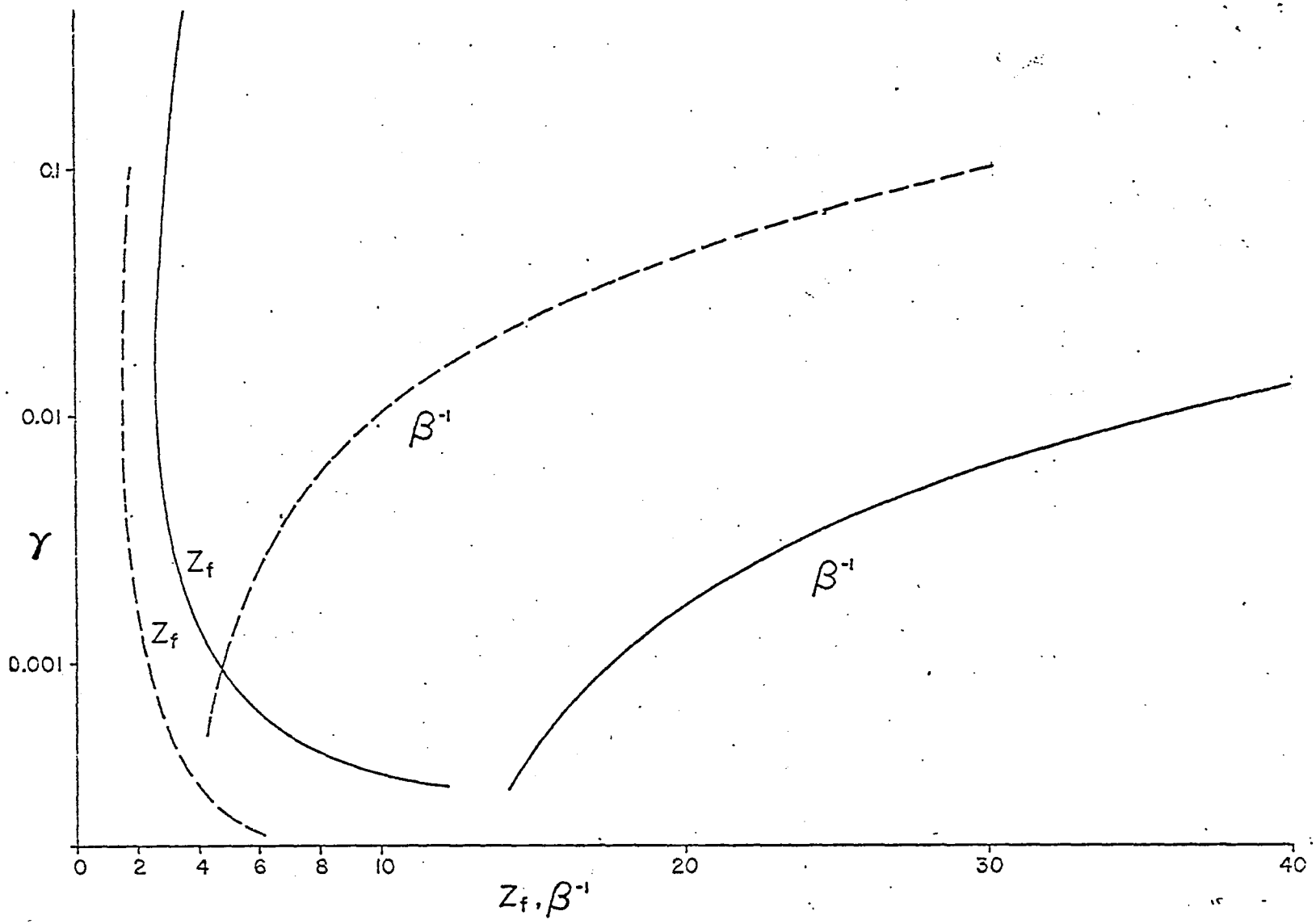

FIG. 5. Focal length z_f and attenuation length β^{-1} as a function of power parameter γ.

Solid line, n= 2.55×10^{15} cm^{-3}; dashed line, n = 6.4×10^{15} cm^{-3}.

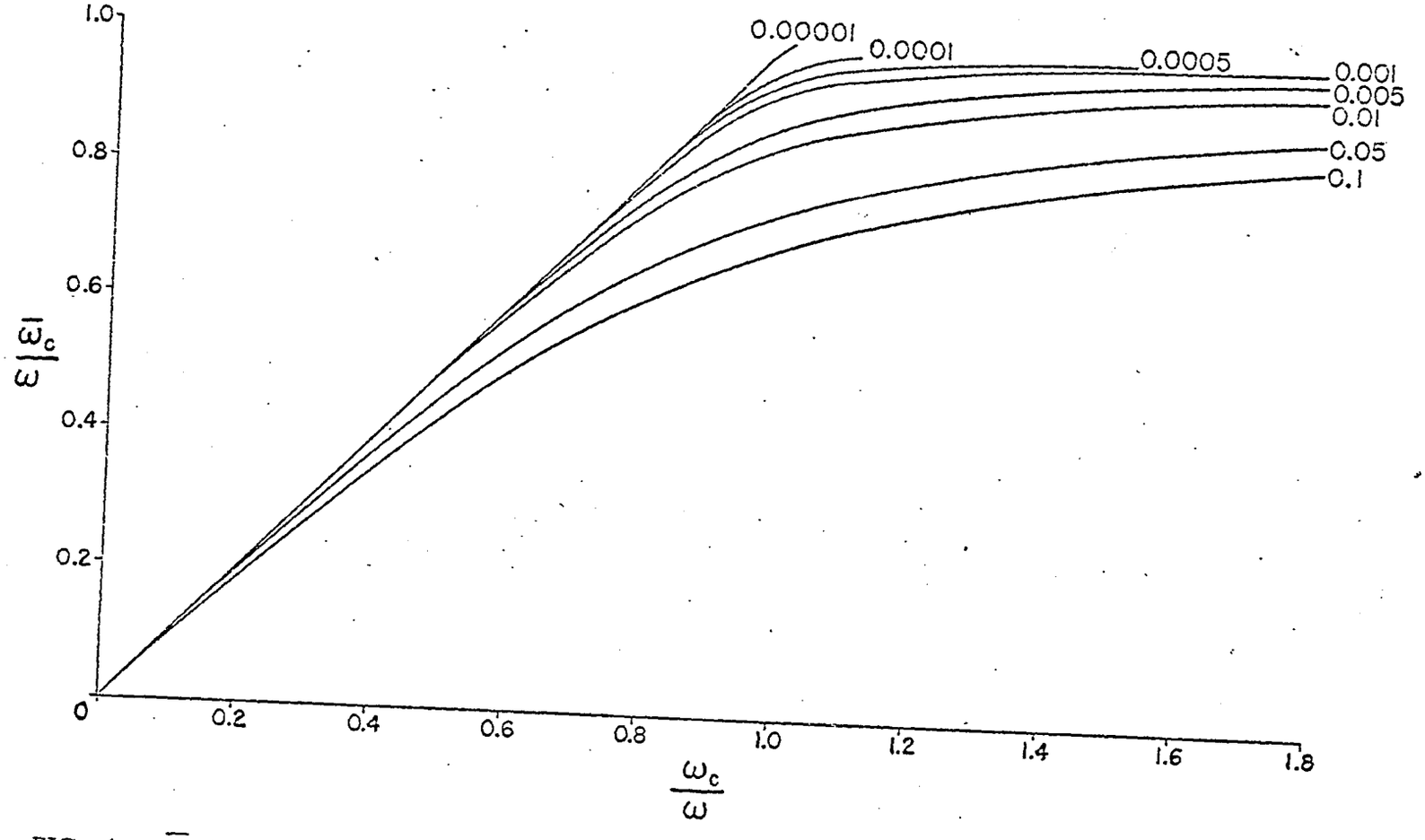

FIG. 6. $\bar{\omega}_c/\omega$ vs. ω_c/ω for different γ values.

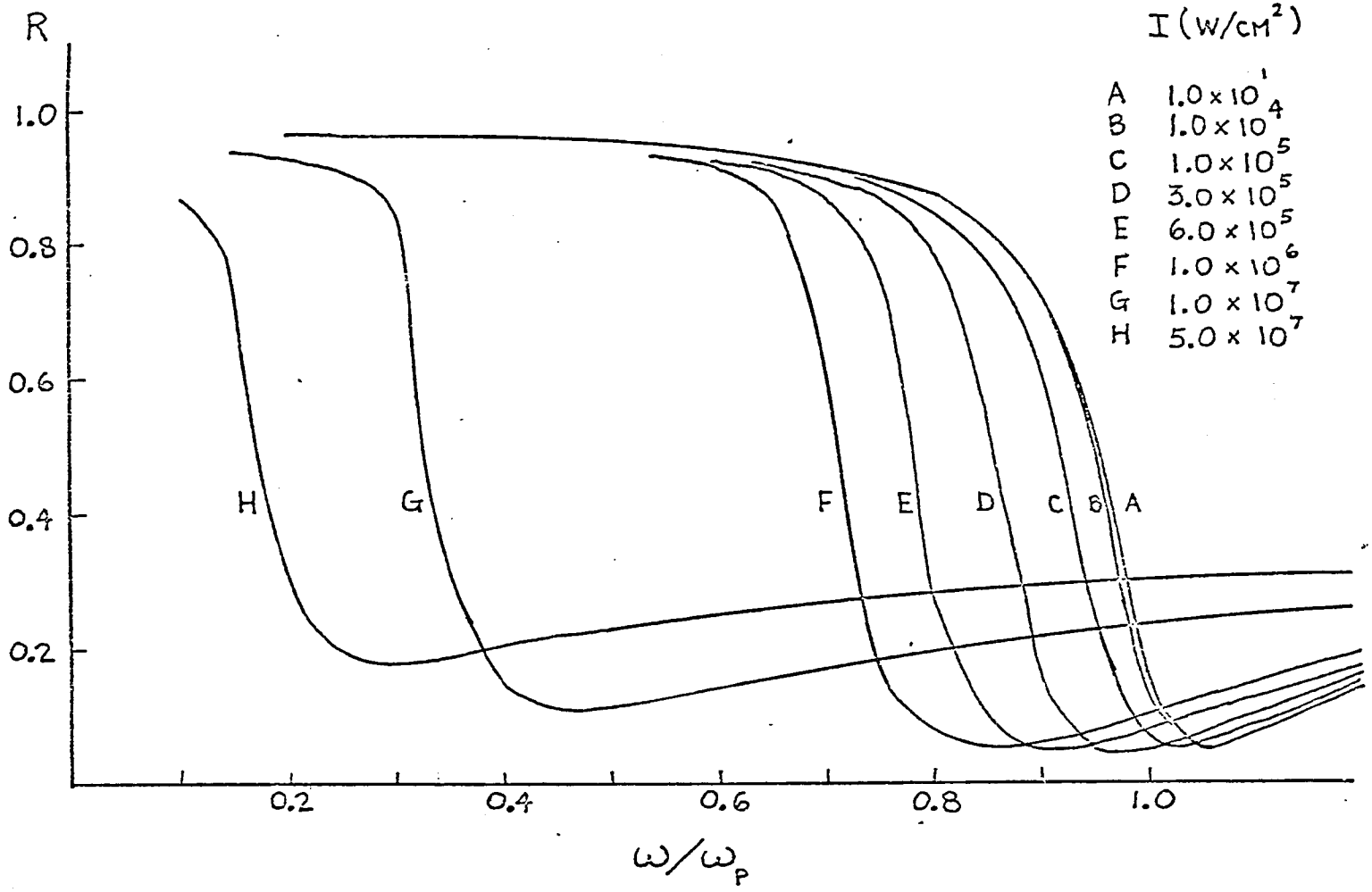

FIG. 7. Reflection efficiency, R vs ratio of laser frequency to plasma frequency, ω/ω_p, for several intensities.

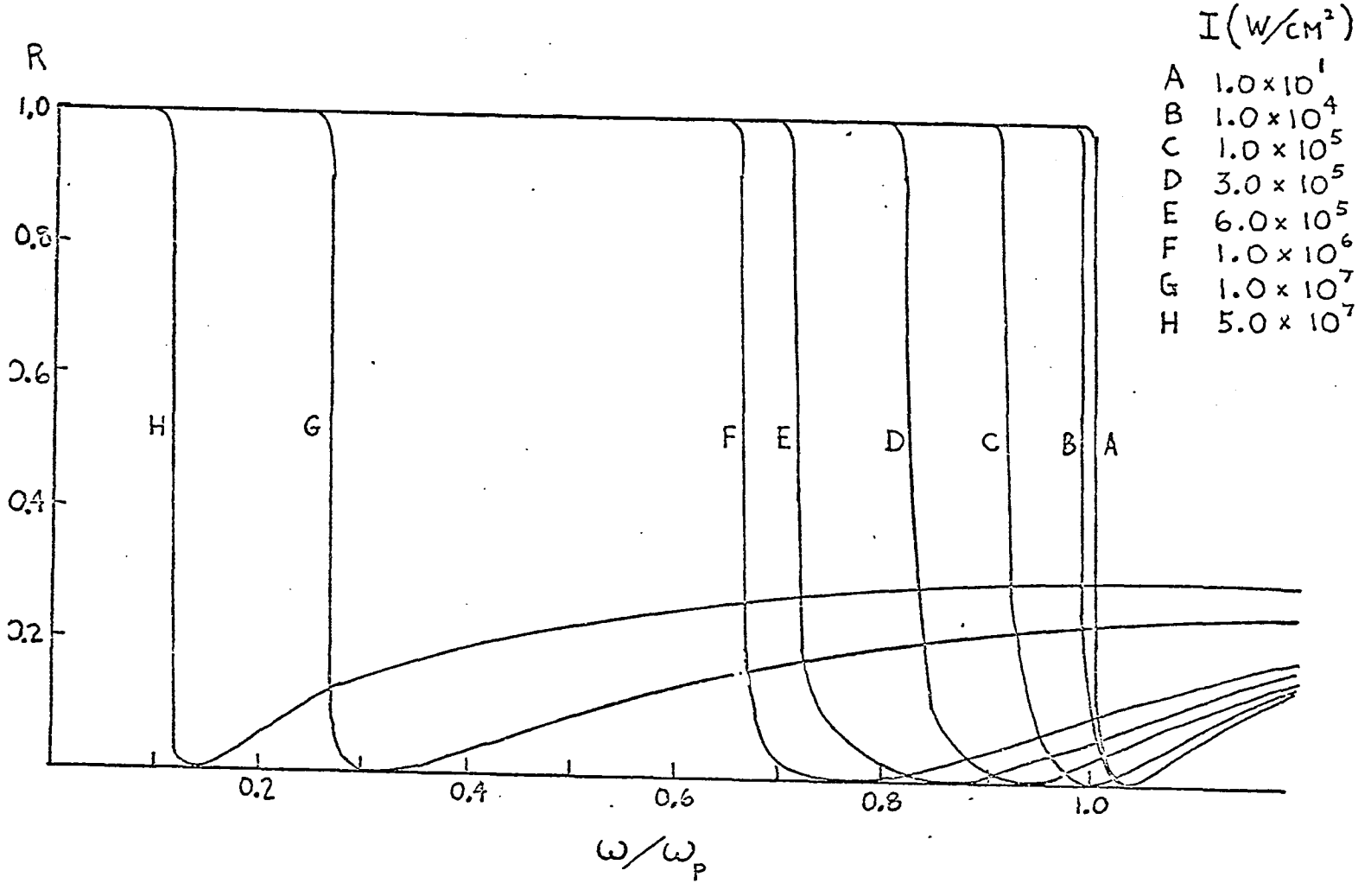

FIG. 8. Same as in Fig. 7 but with collisional effects suppressed.

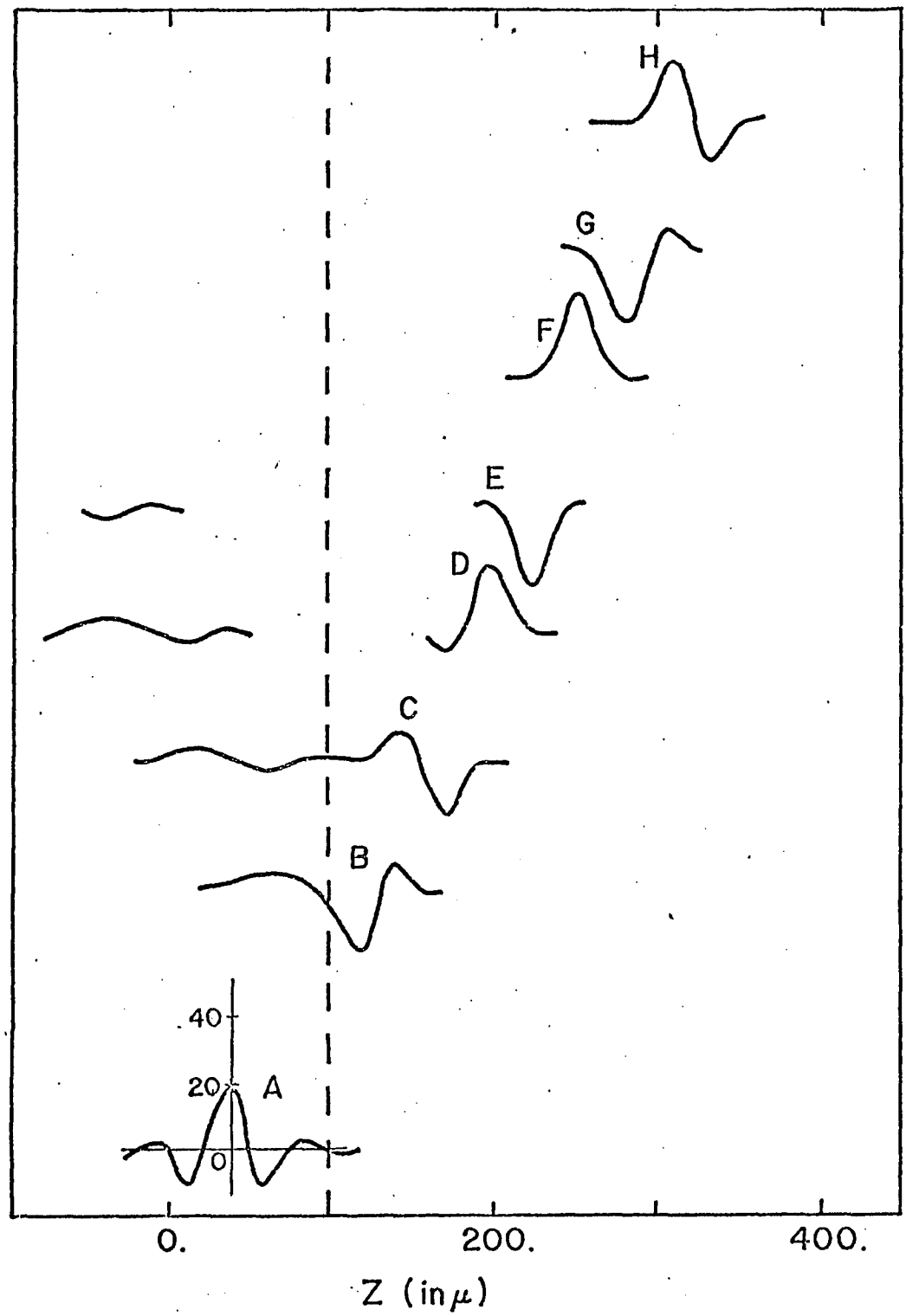

FIG. 9. Profile of pulse impinging on a semi-infinite crystal of doped semiconductor. The doped crystal is to the right of the vertical line. The times at which the pulses are drawn are (in picoseconds): $t_A=0$, $t_B=1.27$, $t_C=1.91$, $t_D=2.5$ $t_E=3.18$, $t_F=3.81$, $t_G=4.45$, $t_H=5.08$. The ratio $\omega/\omega_p = 0.5$. The vertical scale attached to pulse A measures the parameter eA/m^*c^*c.

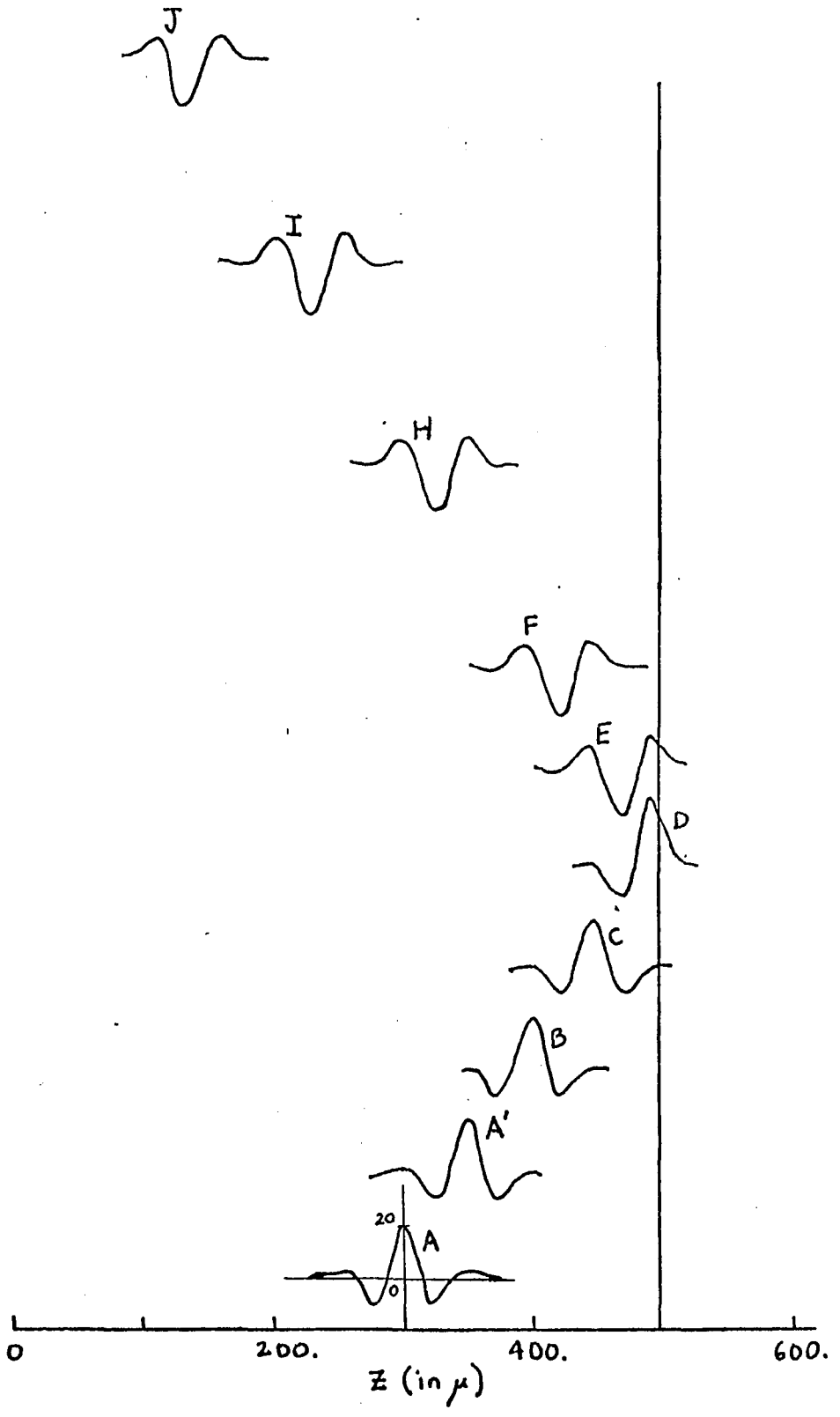

FIG. 10. Same as in Fig. 9 but for a linear plasma rather than a nonlinear plasma. Times corresponding to t_A - t_H are the same as in Fig.9. Also, $t_{A'}$ = .64, t_I =6.35, t_J =7.62 psec.

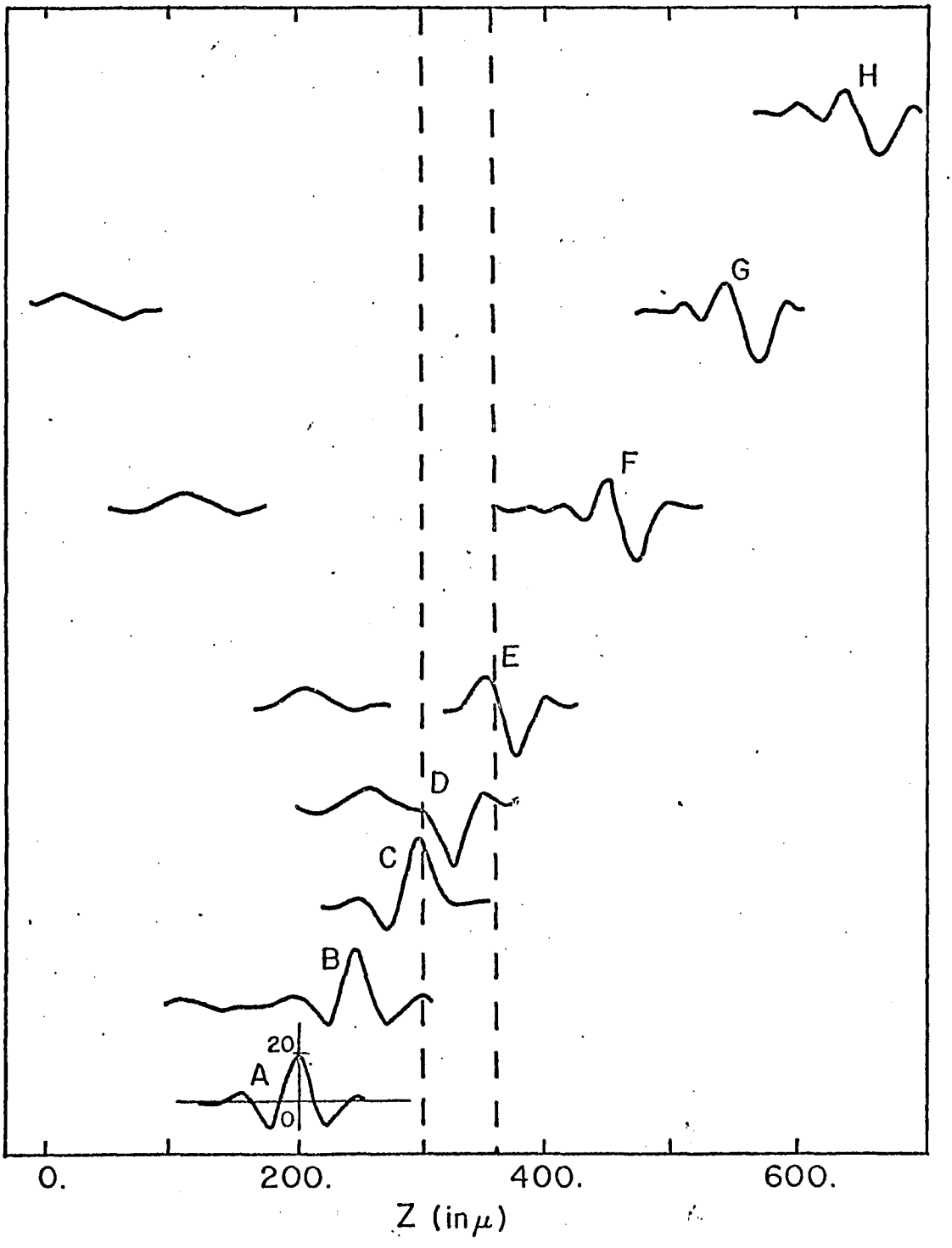

FIG. 11. Self-induced transparency of a doped semiconductor slab of 60 μm thickness. Pulse profile is plotted as a function of z for times (in picoseconds): t_A=0, t_B=.64, t_C=1.27, t_D=1.91, t_E=2.54, t_F=3.81, t_G=5.08, and t_H=6.35.

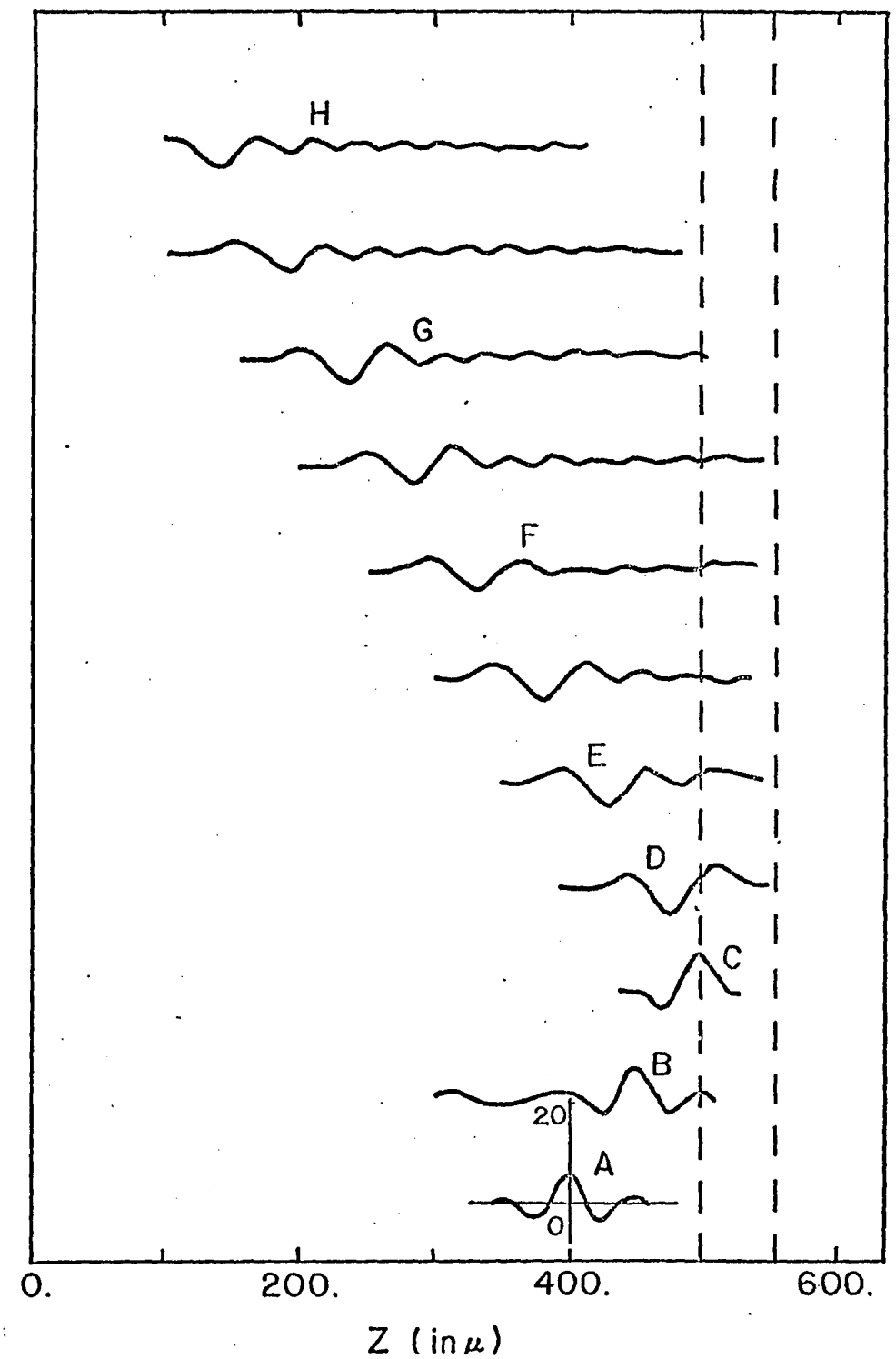

FIG. 12. Same as in Fig. 11 but for a weaker field intensity. The times are the same as in Fig . 11.

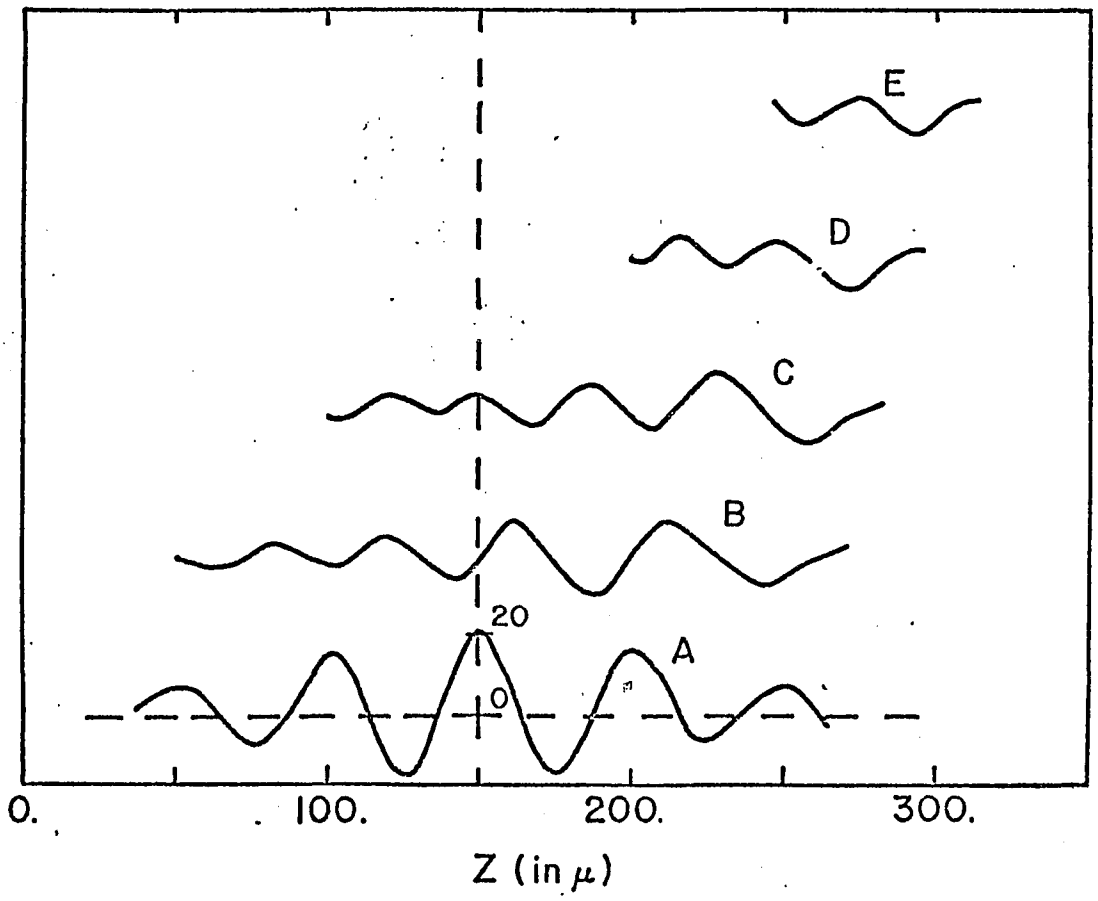

FIG. 13. Propagation of a pulse in a semiconductor including the effect of collisions. The times $t_A - t_E$ are given in Fig. 11.

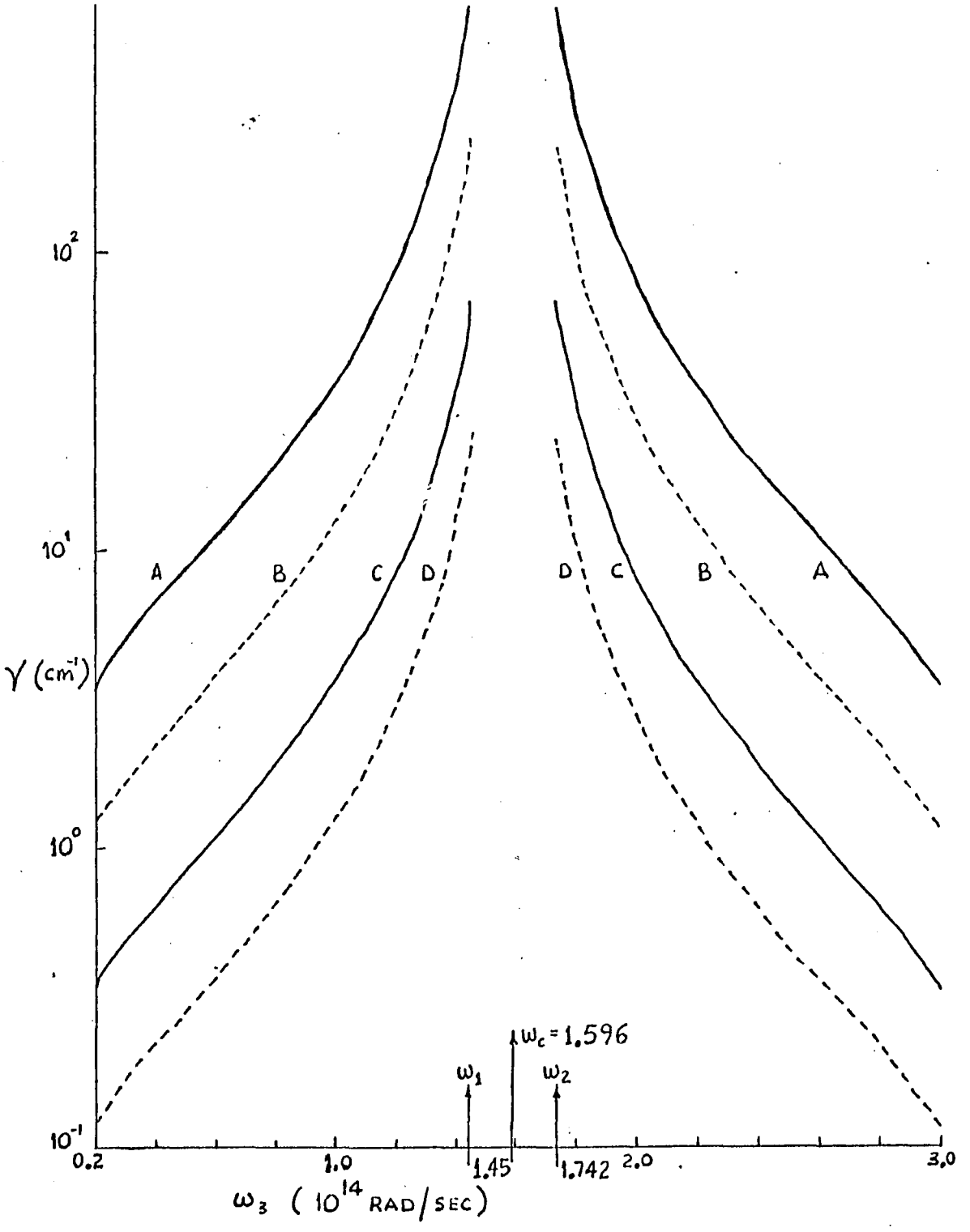

FIG. 14. Growth rate γ vs ω_3 for different intensities I_i and plasma frequencies ω_p. Solid curves, $\omega_p = 3.0 \times 10^{12}$ rad/sec ; broken curves, $\omega_p = 1.742 \times 10^{12}$ rad/sec. Curves A and B, $I_i = 10^7$ W/cm^2; curves C and D, $I_i = 10^6$ W/cm^2.

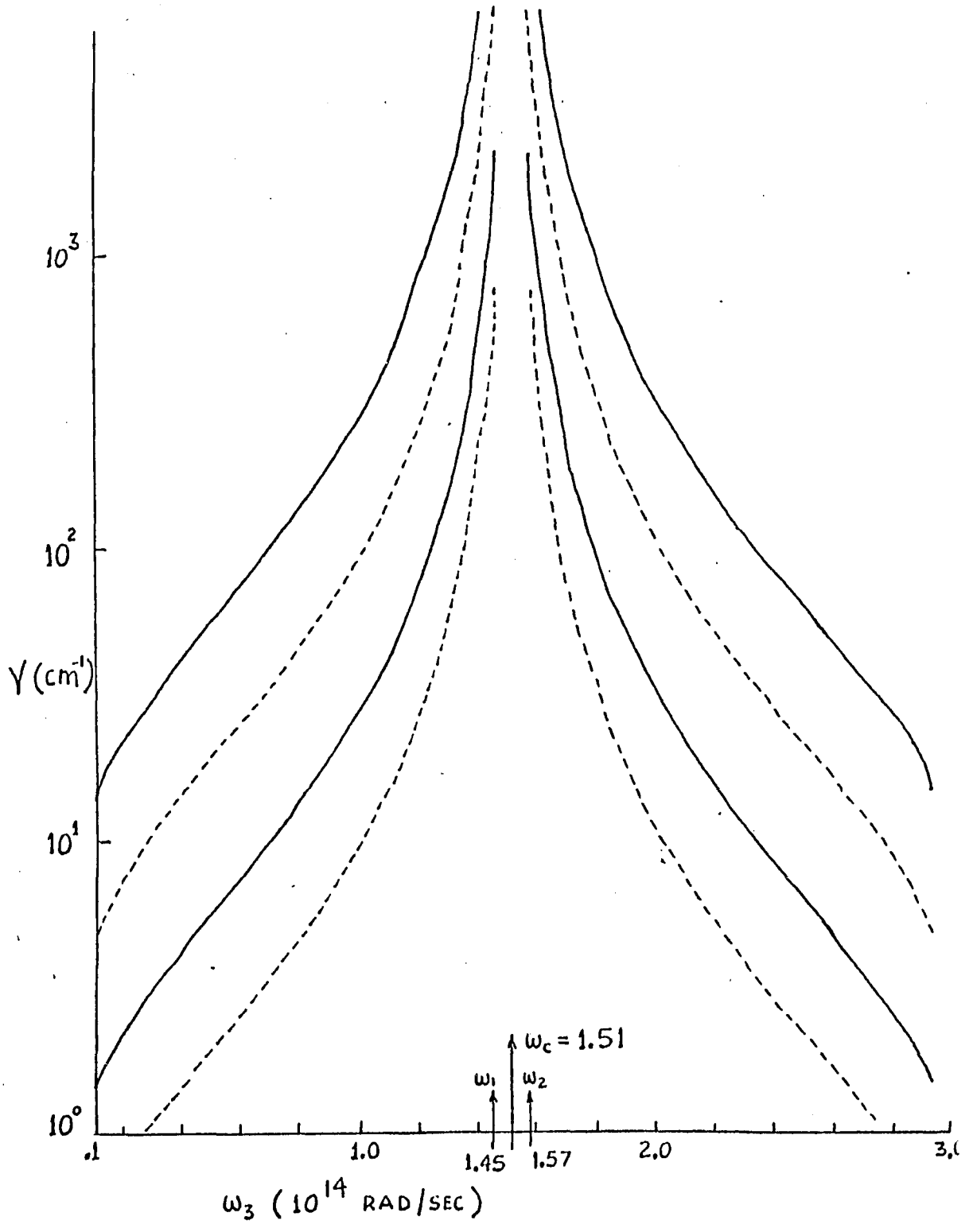

FIG. 15. Growth rate γ vs ω_3 for ω_1, ω_2 and ω_c different from those in Fig. 14. Other parameters are the same as in Fig. 14.

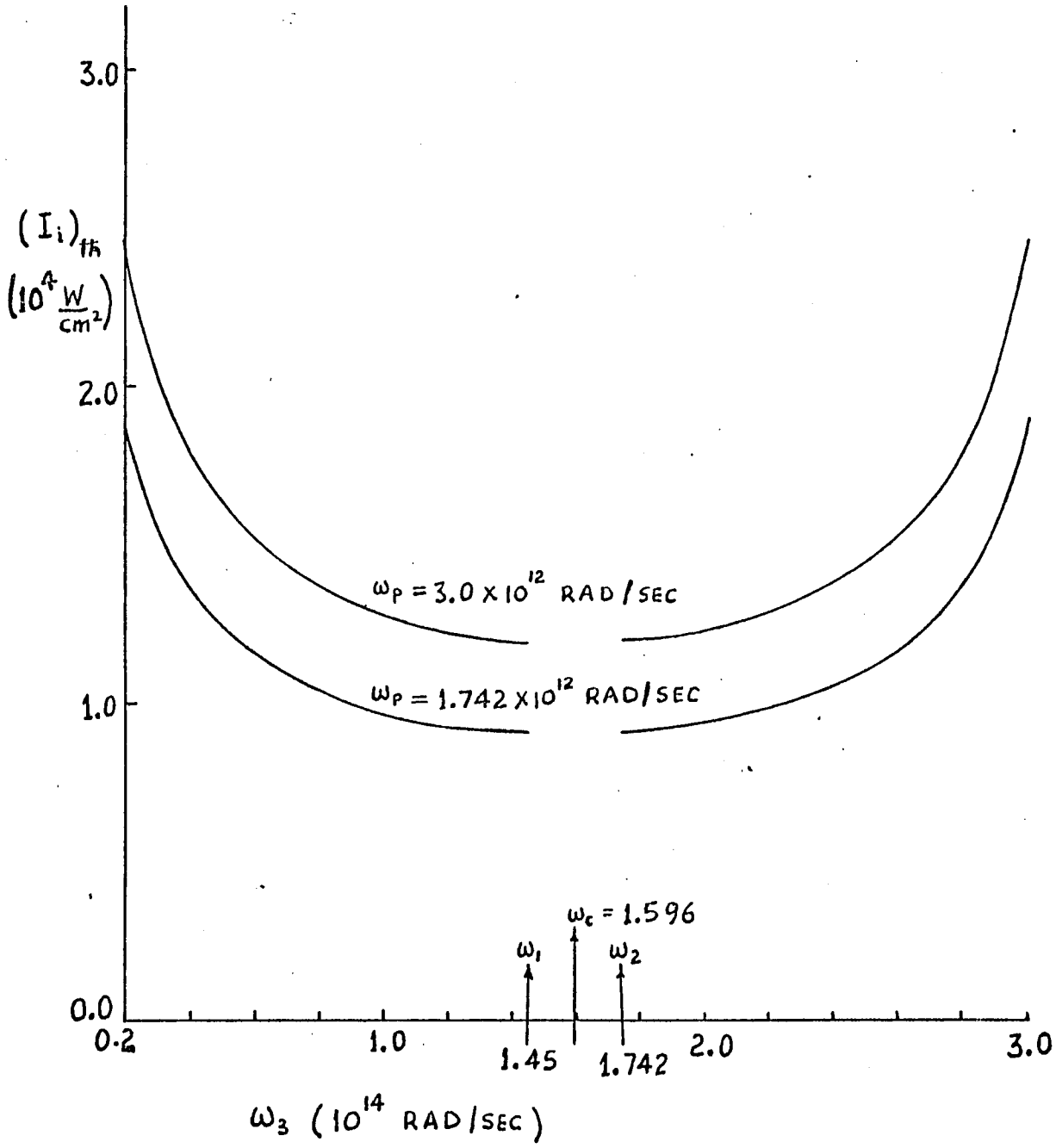

FIG. 16. Threshold intensity $(I_i)_{th}$ vs ω_3 for the same parameters as in Fig. 14.

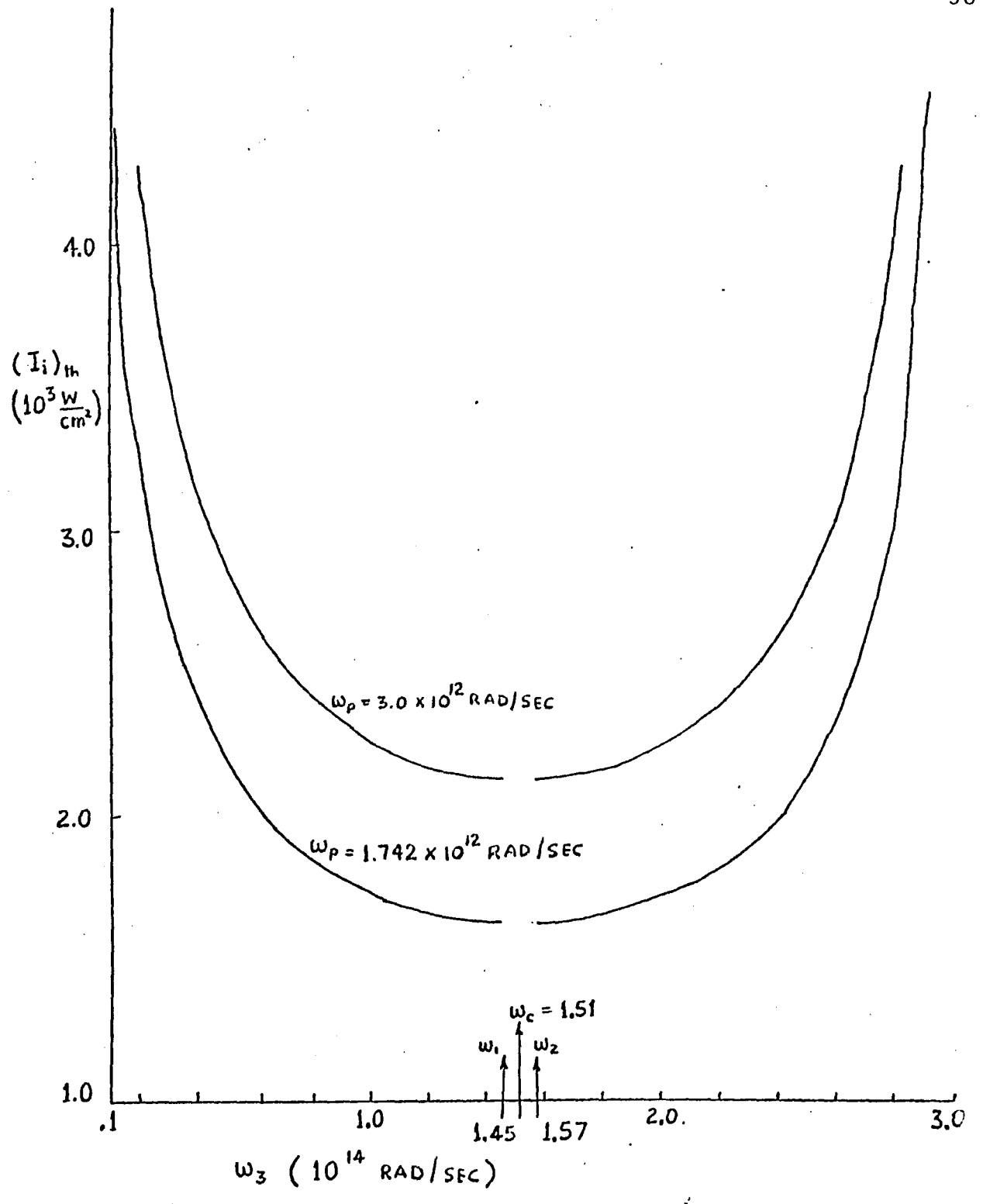

FIG. 17. Threshold intensity $(I_i)_{th}$ vs ω_3 for the same parameters as in Fig. 15.

REFERENCES

1. P. A. Franken, A. E. Hall, C. W. Peters and G. Weinreich, Phys. Rev. Lett., 7, 118 (1961).
2. N. M. Kroll, Phys. Rev., 127 , 1207 (1962).
3. S. A. Akhmanov and R. V. Kokhlov, Soviet Phys., JETP, 16 ,252 (1963).
4. J. A. Armstrong, N. Bloembergen, J. Ducuing and P. S. Pershan, Phys. Rev., 127 , 1918 (1962).
5. A. Yariv, IEEE J. Quant. Elec., 2 , 30 (1966).
6. J. A. Giordmaine and R. C. Miller, Phys. Rev.Lett., 14 ,973 (1965)
7. M. Hercher, J. Opt. Soc. Am., 54 , 563 (1964).
8. R. Chiao, E. Garmire and C. H. Townes, Phys. Rev. Lett., 13 , 479 (1964) ; Phys. Rev. Lett., 14 ,1056 (1964).
9. S. L. McCall and E. L. Hahn, Phys. Rev. Lett., 18 , 908 (1967) ; Phys. Rev., 183 ,457 (1969) ; Phys. Rev., A2 , 861 (1970).
10. C. K. N. Patel and R. E. Slusher, Phys. Rev.Lett., 19 , 1019 (1967)
11. F. Shimuzu, Phys. Rev. Lett.,19 , 1097 (1967).
12. T. K. Gustafson, J. P. Taran, H. A. Haus, J. R. Lifsitz and P. L. Kelley, Phys. Rev., 177,306 (1969) ; F. DeMartini, C. H. Townes, T. K. Gustafson, P. L. Kelley, Phys. Rev., 164 , 312 (1969).
13. F. V. Bunkin and A. M. Prokhorov, Soviet Phys. JETP, 19 , 739 (1964).
14. L. V. Keldysh, Soviet Phys. JETP, 20 , 4 (1965).
15. P. Agostini, G. Barjot, G. Mainfray, C. Manus and J. Thebault, IEEE J. Quant. Elec. 6 , 782 (1970).
16. Y. R. Shen and N. Bloembergen, Phys. Rev., 137 , A1786 (1965) ; N. Bloembergen, Am. J. Phys., 35 , 989 (1967).

17. C. K. N. Patel and E. D. Shaw, Phys. Rev. Lett., 24 , 451 (1970); Phys. Rev., B3 , 1279 (1971).

18. S. A. Akhmanov and R. V. Khokhlov, Problemy Nelineinoi Optiki , (1964), (Problems of Nonlinear Optics, translated by N. Jacobi and R. Sen, Gordon and Breach, New York, 1972).

19. N. Bloembergen, Nonlinear Optics (Benjamin, New York, 1965).

20. P. N. Butcher, Nonlinear Optical Phenomena , (Ohio State Univ. Columbus, 1965).

21. G. C. Baldwin, An Introduction to Nonlinear Optics, (Plenum, New York, 1969).

22. F. Zernike and J. E. Midwinter, Applied Nonlinear Optics , (Wiley, New York , 1973).

23. Quantum Optics , Proceedings of the International School of Physics "Enrico Fermi ", Course XLII, edited by R. J. Glauber (Academic, New York, 1969).

24. Handbook of Lasers , edited by F. T. Arecci and E. O. Schulz- Dubois, (North-Holland, Amsterdam, 1972).

25. Progress in Optics, edited by E. Wolf (North- Holland, Amsterdam, 1961)

26. Progress in Quantum Electronics, edited by J. H. Sanders and S. S. Stenholm (Pergamon, New York, 1969).

27. M. Jain, J. I. Gersten and N. Tzoar, Phys. Rev., B8 , 2710 (1973).

28. N. Tzoar and J. I. Gersten, Phys. Rev. Lett., 26 , 1634 (1971) ; Phys. Rev., B4 , 3540 (1971).

29. M. Jain, J. I. Gersten and N. Tzoar, Phys. Rev., B10 , 2474 (1974).

30. M. Jain, J. I. Gersten and N. Tzoar, J. Appl. Phys., 46, 3969 (1975).

31. N. F. Pilipetskii and A. R. Rustamov, Soviet Phys. JETP Lett., 2, 55 (1965).

32. R. Chiao, E. Garmire and C. Townes, Phys. Rev. Lett., 13 , 479 (1964) ; Phys. Rev. Lett.,14 , 1056 (1965) ; Phys. Rev. Lett. 16, 347 (1966).

33. S. A. Akhmanov, A. P. Sukhorukov and R. V. Khokholov, Soviet Phys. Usp., 10 ,609 (1968).

34. M. Maier, G. Wendl and W. Kaiser, Phy. Rev. Lett., 24,352 (1970).

35. M. M. T. Loy and Y. R. Shen, Phys. Rev. Lett.,14 , 380 (1969).

36. D. Grishkowsky, Phys. Rev. Lett., 24 , 866 (1970).

37. P. K. Dubey and V. V. Paranjape, Phys. Rev., B6 , 1321 (1972).

38. M. S. Sodha, D. P. Tewari, J. Kamal and V. K. Tripathi, J. Appl. Phys., 43 , 3736 (1972).

39. E. O. Kane, J. Phys. Chem. Solids, 1 , 249 (1957).

40. H. Goldstein, Classical Mechanics , (Addison- Wesley, Reading, Mass.,1959).

41. C. Hilsum and A. C. Rose, Semiconducting III-V Compounds (Pergamon, New York, 1961) ; Semiconductors and Semimetals , edited by R. K. Willardson and A. C. Beer (Academic, New York 1966).

42. H. M. Gibbs and R. E. Slusher, Phys. Rev. Lett.,24 , 638 (1970).

43. C. Max and F. Perkins, Phys. Rev. Lett.,27 , 1342 (1971).

44. N. Tzoar and J. I. Gersten, Phys. Rev. Lett.,28 , 1203 (1972).

45. F. D. Tappert and C. M. Varma, Phys. Rev. Lett.,25 , 1108(1970).

46. I. S. Gradshteyn and I. W. Ryzhik, Tables of Integrals , Series and Products,(Academic , New York, 1965).

47. In InSb, the dominant nonlinearity is due to nonparabolicity and not such effects as energy dependent collision times. See C. C. Wang W. W. Ressler, Phys. Rev., 188 , 1291 (1961) ; K. C. Rustagi, Phys. Rev., B2 , 4053 (1970).

48. J. I. Gersten and N. Tzoar, Phys. Rev., B6 , 1375 (1972).

49. R. E. Slusher, C. K. N. Patel and P. A. Fleury, Phys. Rev. Lett., 18 , 77 (1967).

50. C. K. N. Patel in Laser Spectroscopy , edited by R. G. Brewer and A. Mooradian (Plenum, New York, 1973), p. 471.

51. J. F. Scott, T. C. Damen and P. A. Fleury, Phys. Rev., B6, 3856 (1972).

52. R. L. Hollis, J. F. Ryan and J. F. Scott, Phys. Rev. Lett., 34 , 209 (1975).

53. J. A. Giordimaine in Ref. 23, p.493.

54. F. DeMartini and P. L. Kelley in Ref. 23 , p. 574.

55. M. Jain and N. Tzoar, Phys. Rev., B10 , 5159 (1974).